APPLICATION OF HYBRID FINITE ELEMENT METHOD TO FIND INTERLAMINAR STRESSES IN COMPOSITES

A Thesis Submitted
in Partial Fulfilment of the Requirements
for the Degree of

MASTER OF TECHNOLOGY

by

ANIRUDDHA CHAHANDE

to the

DEPARTMENT OF MECHANICAL ENGINEERING
INDIAN INSTITUTE OF TECHNOLOGY KANPUR

OCTOBER, 1989

cert. bd.

CERTIFICATE

This is to certify that the work entitled "Application of Hybrid Finite Element Method to Find Interlaminar Stresses in Composite" by Aniruddha Chahande has been carried out under my supervision and has not been submitted else where for a degree.

NN Kishore 9/10/95

Dr. N. N. KISHORE
Assistant Professor
Department of Mechanical Engineering
Indian Institute of Technology
Kanpur, 208 016

A C K N O W L E D G E M E N T S

I am extremely grateful to Dr. N. N. Kishore for his valuable guidance and constant encouragement at all stages of this work.

A million thanks are due to Anil for his helping hand in drawing diagrams and entering the data for my program. Thanks to D. K. and Tillu for their assistance. I would like to express my gratitude to all ESA-Lab people for their support and company at all stages of my work. Also thanks to all my friends who made my stay at IIT-K a pleasant and memorable one.

(Aniruddha Chahande)

CONTENTS

LIST OF SYMBOLS

X_1, X_2, X_3	Material co-ordinate system
x, y, z	Global co-ordinate system
θ	Angle between material co-ordinate system and global co-ordinate system
σ^i	Vector of stresses for layer i
$\hat{\varepsilon}^i$	Vector of stresses in layer i
$\underline{u}^i$	Displacement vector of layer i
S^i	Material property matrix relation stresses to strains
$\underline{T}^i$	Prescribed tractions
V_{n_i}	Volume of layer i
$S_{\sigma_{n_i}}$	Portion of element boundary on which tractions are prescribed
I	Total number of layers in laminated composite
E_{11}, E_{22}	Young's moduli in the fibre and transverse to fibre directions respectively
ν_{12}, ν_{23}	Major and minor Poisson's ratio respectively
P^i	Matrix which contents typical set of polynomials used for stress assumptions

$\underline{\beta}^i$	Constants used in stress assumptions
$N_j(\xi,\eta)$	Biquadratic Serendipity shape functions
ξ, η, ζ	Are the normalized co-ordinate system
$\underline{q}^i$	Nodal displacements of layer i
N^i	Shape functions in normalized co-ordinate (ξ,η,ζ)
D^i	Strain displacement differential operator matrix
$\|J\|$	Jacobian for co-ordinate transformation
$\bar{t}_i$	Half the thickness of layer i
K	Elemental stiffness matrix
Q	Elemental load vector
C_β^i	Matrix which relates layer stress parameters β^i to laminate stress parameters β
C_q^i	Matrix which relates layer nodal displacements q^i to laminate nodal displacements q

LIST OF FIGURES

SYNOPSIS

The present work concerns with an analysis of edge stresses in symmetric cross-ply laminates under uniform farfield strain. The problem has been considered in view of the increasing applications of multilayered composites in the field of aerospace and aircraft structures, and the delamination failure of these multilayered composites due to high interlaminar stresses.

Similar problems were solved by the application of semi-analytical methods or displacement based finite element method. The analytical methods are complex in their formulation and solution procedures. Displacement based FEM solution have slow convergence and requires the use of very fine mesh and large computing time. The hybrid FEM offers better convergence as they involve assumption of stress functions closer to the actual variation. Further the difficulty of sever stiffening in thin plate limit and/or spurious zero energy modes are avoided by judicious use of hybrid-stress finite element model. The simplicity and application of hybrid elements for analysis of stresses provide the necessary insight for their application to present problem.

A hybrid stress 8-node isoparametric multilayered plate elements were chosen to solve the present problem of interlaminar edge stresses near a straight boundary, circular hole boundary and square hole boundaries. The hybrid stress model is based on modified complementary energy principle and takes into account the transverse deformation effects. All the three displacements

components are assumed to vary linearly through the thickness of each lamina and the stress components are included and are interpolated independently within each layer; they also satisfy equation of equilibrium.

A program is developed based on above theory to solve the present problem. The results show that there is a possibility of mode-I delamination near straight edges and mixed mode delamination near circular hole and square hole boundaries.

CHAPTER I

INTRODUCTION

1.1 GENERAL INTRODUCTION

1.1.1 Composite material

The word composite means 'consisting of two or more distinct parts'. Thus materials having two or more distinct constituents, on a macroscale having distinct interface separating them are called composite materials [Agarwal and Broutman(1980)]. The composites achieve certain physical properties not realizable by the constituent materials, such as high specific strength and stiffness and controlled anisotropy. Composite structures have many applications, specially in aerospace and transport industry due to their properties such as good fatigue and corrosion resistance, low heat conductivity, good electrical insulation properties, favorable cost effectiveness etc.. Also in the recent past extensive research on the manufacture, characterization, fatigue and fracture of these materials have increased the confidence in the use of these materials.

1.1.2 Interlaminar Stresses/Free-Edge Effects

A characteristic of laminated composites is that under inplane uniaxial or biaxial loading conditions, a laminate often develops triaxial effects near edges i.e. depending on its lay-up,

a laminate under inplane loading develops out-of-plane stresses. These out-of-plane stresses are known as 'Interlaminar Stresses' [Agarwal and Broutman (198Ø)]. Their effect is more significant near free-edges where some stress components may attain high values. The interlaminar stresses are regarded as an edge-effect [Pipes and Daniel (1971)], or boundary layer effects, since their effect is confined to a narrow region close to edges, of the order of the laminate thickness. A tensile value of interlaminar normal stress σ_z at free-edge may initiate delamination and thus accelerate the failure process. Thus, interlaminar stresses are one of the mechanisms that leads to delamination failure in composite laminates.

Due to the functional or design requirements, the mul-tilayered laminates may contains holes, cut-out etc. which in addition to edges on sides of laminates act as free edges. From the view point of delamination analysis, the magnitude and nature of interlaminar stresses at free-edges are very important. The stacking sequence in laminate affects magnitude as well as the nature of interlaminar stresses [Pagano and Pipes (1971)].

1.2 LITERATURE SURVEY

The first direct approach to the problem of interlaminar stresses have been made by Puppo and Evensen (197Ø). They developed an approximate formulation in which the laminate was modeled as a set of anisotropic layers separated by an isotropic adhesive layers. A second solution was developed by Pipes and Pagano (197Ø), for a four layer symmetric angle-ply laminate under

uniform axial extension by assuming that the stress components are independent of longitudinal direction. The theoretical results of Pipes and Pagano (1970) were experimentally confirmed by Pipes and Daniels (1971). They confirmed that the interlaminar stresses can be regarded as edge-effect since their effect is confined to a region whose width is equal to the laminate thickness. Pagano and Pipes (1971) demonstrated that the interlaminar stresses can be significantly influenced by the laminate stacking sequence, and thus stacking sequence may be important to designer.

An approximate method which takes into consideration the influence of the pertinent material and geometric parameters on the variation of the interlaminar normal stresses along the central plane of the symmetric finite width laminate has been presented by Pagano (1974). An approximate elasticity solution has been developed by Pipes and Pagano (1974) for the response of finite width, symmetric angle-ply laminate under uniform axial strain. Tang (1976) derived the governing differential equations for uniformly loaded rectangular composite plate using classical lamination theory and approximate boundary conditions. Tang (1977) used a boundary layer theory to obtain stress distributions around circular hole in $[0/90]_s$ and $[\pm 45]_s$ laminates, but he used extremely large value of 400 for the ratio of hole radius to ply thickness.

Pagano (1978) reduced the free-edge class of boundary value problem to a one-dimensional problem to predict stress fields in composite laminate. For n-layered laminate, the solution involves consideration of 13n algebraic and ordinary differential equations and the theory is specialized for the case

of symmetric laminates.

Kassapoglous and Lagace (1986) have presented a method which predicts three dimensional stress state in laminated composites. Expressions for the interlaminar stresses have been assumed in terms of exponentials based on shapes that the interlaminar stresses must take in order to assure force and moment equilibrium. The boundary and traction continuity between plies are satisfied exactly. Chaudhuri and Seide (1987) have presented an approximate semi-analytical method to determine transverse shear stress variation across the thickness.

A three-dimensional finite difference solution for the problem of free edge effects in uniaxially loaded, symmetric angle-ply laminates has been presented by Altus et al. (198Ø).

A Finite element model has been developed by Isakson and Levy (1971) to determine the interlaminar stresses for generalized plane stress conditions and is based on the concept used earlier by Pipes and Pagano (197Ø). Rybicki (1971) has presented a three-dimensional finite element formulation using complementary energy approach. An Approximate solution has been presented for symmetric laminate under inplane loading. Wang and Crossman (1977) have presented finite element formulation that include mechanical (uniaxial tension), thermal and hygrothermal load, and presented results for symmetric finite width laminate under uniaxial tension. The formulation is based on generalized plane strain approach. Wang and Dickson (1978) applied the extended Galerkin's method with displacements and interlaminar stresses represented by complete set of Legendre polynomials.

Lee (198Ø) has adopted 8-noded brick element having three

degrees-of-freedom per node for three-dimensional finite element analysis of symmetric composite laminate with a center hole and subjected to biaxial inplane loads. The finite element formulation using 8-noded isoparametric element has been described by Raju and Crews (1981) to analyse the free edge stress problem of 4-ply composite laminate. The existence of stress singularities at the free-edges has been investigated. They have also analysed edge stresses near the boundary of circular hole in a symmetric cross-ply laminate [Raju and Crews (1982)], where-in they have used 19000 degrees-of-freedom to obtain the edge stresses. Rohwer (1982) has used three-dimensional finite element to evaluate the edge stresses in the symmetric laminate.

Pian (1973) developed the hybrid element and showed that because of high accuracy of hybrid elements, they are more efficient than the assumed displacement elements

In recent past Spilker et. al. have developed hybrid stress formulation to analyse various types of plate problems, based on different assumptions. Spilker and Chow (1980) have analysed symmetric cross-ply laminates under uniform inplane strain using finite element technique based on a hybrid-stress approach in which equilibrium in each layer, continuity of appropriate stresses and displacements at interfaces between layers, and traction-free condition have been satisfied exactly. Spilker and Munir (1980-1) developed an assumed stress finite element model for the analysis of bending of thin plates. A hybrid stress functional is defined by using Mindline-type displacement assumption. They also developed (1980-2) a hybrid stress element for the analysis of thin and moderately thick

plates. They have shown that this hybrid stress element yields superior accuracy as compared to assumed displacement based Mindline plate element with reduced integration. Spilker (1980) developed a hybrid stress based finite element formulation for thick multilayer laminates where in attention is restricted to cylindrical bending of cross-ply laminates and two-dimensional plane-strain element. He has developed (1982) hybrid stress 8-node isoparametric multilayer plate element for the analysis of thin to thick fibre-reinforced composite plates. In present work this element is used to analyse the edge stress problem. Wang and Yuan (1983) have developed a finite element formulation for solving the boundary layer problem based on the elasticity theory and the modified principle of hybrid variational function. The advanced hybrid, singular element used in conjugation with conventional isoparametric quasi-three-dimensional elements have been shown to be especially suitable for examining the exact and detailed nature of boundary layer stresses in composite laminates.

1.3 SCOPE OF PRESENT WORK

The purpose of the present study is to estimate the interlaminar edge stresses in the vicinity of straight edge boundary, circular hole boundary and square hole boundaries. The basic understanding of three dimensional stresses at laminate hole is addressed.

The present study focused on four ply-laminate with $[0/90]_s$ and $[90/0]_s$ stacking sequence. A large laminate with a central hole is considered for the present analysis. The

dimensions of length and width with respect to the hole size are chosen such that the plate can be considered infinite.

In present work hybrid stress 8-node isoparametric multilayer plate element [Spilker (1982)] is used to analyse the edge stresses near the boundary of hole, in a symmetric cross-ply laminate under uniform far field strain conditions. The feasibility of computer implementation and validity of the results are checked.

Chapter II deals with formulation of problem, taken for present work.

Chapter III briefly describes, the concept of hybrid FEM, and its application to analysis of edge stresses in a fibre-reinforced composites. It also includes the programme structure and related important features of program development.

In Chapter IV results are included and discussed.

Chapter V presents conclusions drawn and suggestions for further work.

CHAPTER II

PROBLEM DEFINITION

This chapter explains nature of problem under consideration. It also deals with various types of assumption and boundary conditions used while analysing the present problem.

Fig. 2.1 shows a four ply-laminate with each ply having thickness of h. It has a central circular hole of radius R. The laminate is subjected to a uniform far field displacements in y direction. Each ply is idealized as homogeneous, elastic, orthotropic material with properties as given below:

$$E_{11} = 20 \times 10^{6} \text{ Psi } (138 \text{ GPa})$$

$$E_{22} = 2.1 \times 10^{6} \text{ Psi } (14.5 \text{ GPa})$$

$$G_{12} = 0.85 \times 10^{6} \text{ Psi } (5.86 \text{ GPa})$$

$$G_{23} = 0.85 \times 10^{6} \text{ Psi } (5.86 \text{ GPa})$$

$$\nu_{12} = 0.21$$

$$\nu_{23} = 0.21$$

The subscripts 1, 2 and 3 denote the longitudinal, transverse and thickness direction respectively of individual ply.

Because of symmetries in the problem, only one eighth of the laminate was analysed (Fig. 2.1) with following boundary conditions.

i) Displacement boundary condition

a) $u = 0$ on $x = 0$

$v = 0$ on $y = 0$

$w = 0$ on $z = 0$

b) On the far end y = 1 plane

$$u = u_o \text{ (constant)}$$

ii) Traction boundary conditions:

a) The edges x = b
   The top surface z = 2h
   } Traction free

b) The hole boundary r = R is traction free.

The analysis is aimed at obtaining the stress distribution in the idealized laminate caused by the above mentioned loading. Because of complexity in satisfying the equation of equilibrium, compatibility conditions and the boundary conditions, of orthotropic elasticity, exact solutions are difficult to obtain. In the present work, hybrid finite element method [Spilker (1982)] is used to obtain the stress distributions in the laminate and in particular near the free edges.

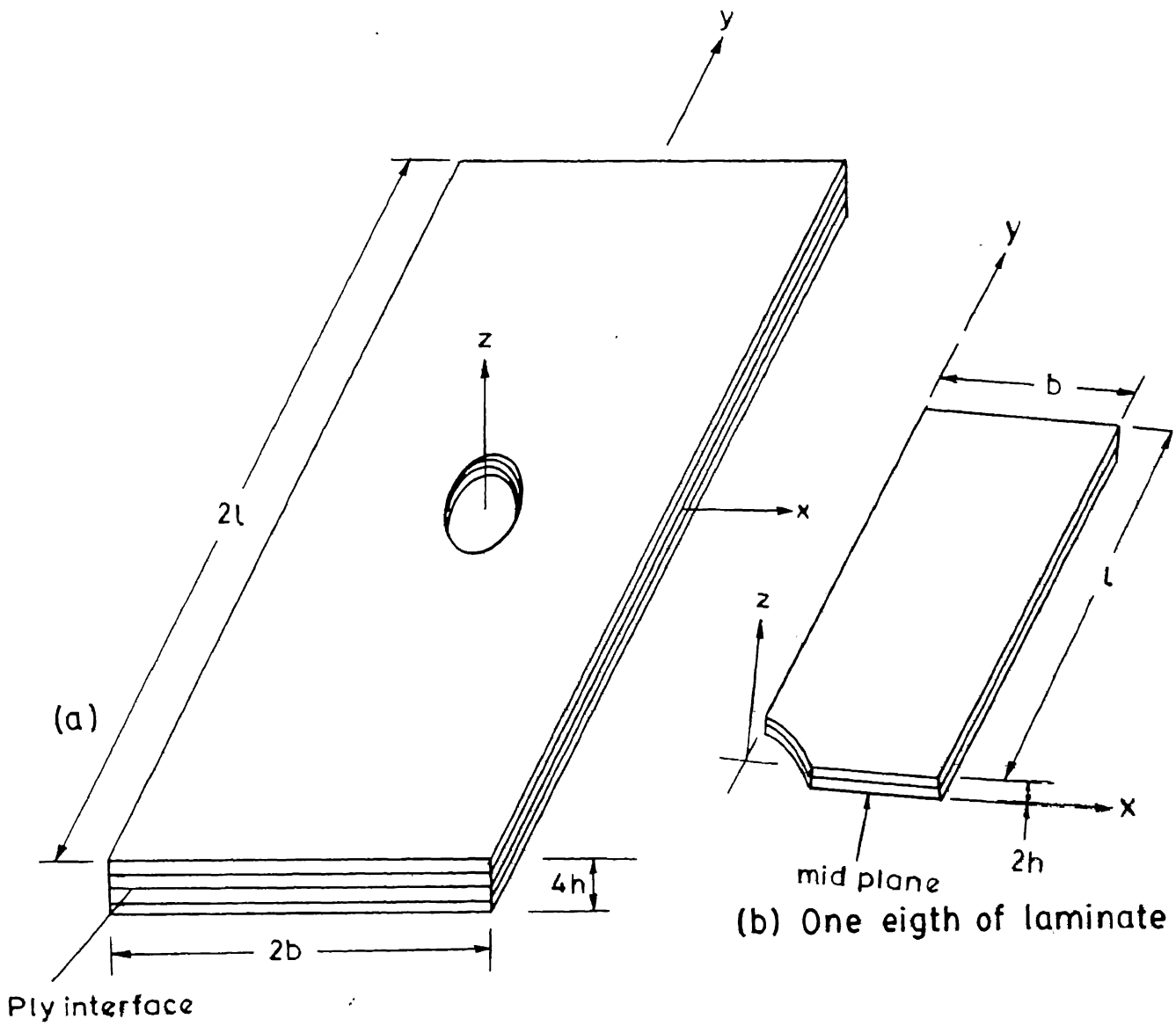

FIG. 2.1 GEOMETRY OF LAMINATE WITH HOLE

CHAPTER III

THE HYBRID FEM APPROACH APPLIED TO LAMINATED PLATES

3.1 INTRODUCTION

Consider the solution of linear boundary value problem by FEM. If we apply the principle of minimum potential energy to such a finite element assemblage, it is evident that the assembled displacement field in the element should be such that it is not only continuous within the element but also compatible at the interelement boundaries. The variational principle then leads to equations, which satisfy (a) equilibrium within the element and (b) interelement traction condition. Similarly in application of complementary energy principle, it is seen that the admissible stress field should, be eqilibrated within each element and satisfy the interelement traction condition, and the complementary energy principle then leads, to (a) kinematic compatibility within element and (b) displacement compatibility between elements.

The above requirements of interelement displacement continuity and traction condition on admissible displacement and stress fields respectively may not provide sufficient flexibility in finite element solution of several problems in linear solid mechanics, such as plate bending, shells, multilayer composites, problem involving singularities, fracture mechanics problems etc.

To gain flexibility, in application, one may relax the condition of displacement continuity and/or traction condition at interelement boundaries, on admissible displacement or stress

fields. For doing this one has to introduce the posterior constraints to respective finite element variational principle through Lagrange constraint fields, at interelement boundaries. This is the underlying concept of the Hybrid FEM.

3.2 DEFINITION OF ELEMENT STIFFNESS MATRIX

The elements considered here are assumed to lie in x-y plane with z corresponding to the transverse direction. The element is composed of I perfectly-bonded layers of transversely isotropic material. The layers and I+1 surfaces (interlayer surfaces and lower/upper laminate surfaces) are numbered from bottom to top of the laminate. The origin of the reference surface, z = Ø, is at the bottom and location of each surface is given by $z = h_1(h_1=\emptyset), h_2, \ldots, h_{I+1}$ (see Fig. 3.1). Each layer is of constant thickness and constant material properties (i.e. material constants in the material axis system, and ply/fibre orientation angle, θ), but thickness and properties may vary from layer to layer.

The elements [Spilker (1982)] used in present problem are based on hybrid-stress model. This model uses a modified complementary energy principle in which interelement traction continuity and mechanical boundary condition have been relaxed via the Lagrange multilayer technique. The hybrid stress functional for multilayer element can be expressed as

$$\pi_{mc} = \sum_{n} \sum_{I} \left\{ \frac{1}{2} \int_{V_n} \underline{\sigma}^{i^T} \underline{S}^i \underline{\sigma}^i dV - \int_{V_n} \underline{\sigma}^{i^T} \hat{\underline{\varepsilon}}^i dV + \int_{S_n} \underline{u}^{i^T} \overline{\underline{T}}^i dS \right\} \qquad (1)$$

where $\underline{\sigma}^i$ is the vector of stresses for layer i, $\hat{\underline{\varepsilon}}^i$ is the vector of strains in layer i computed (via strain-displacement relations) from displacements, $\underline{u}^i$, S^i is the material property matrix relating stresses to strains (i.e. $\underline{\varepsilon}^i = S^i \underline{\sigma}^i$, where $\underline{\varepsilon}^i$ are actual strains, to be distinguished from $\hat{\underline{\varepsilon}}^i$), $\underline{T}^i$ are prescribed tractions, V_{n_i} is volume of layer i for element n, and $S_{\sigma_{n_i}}$ is the portion of element boundary on which tractions are prescribed. The inner sum is over layers of element n, and the outer sum is over the number of elements.

If the stresses are assumed to satisfy equilibrium in each layer (as required in the hybrid stress model) and tractions are required to be continuous across interlayer surfaces (as required in the present multilayer element formulation), the volume integral is replace by a surface integral, over the exterior surfaces of the element of tractions (from stresses) times displacements, as found in conventional statements of π_{mc}.

Each layer of the multilayer element consists of a fibre reinforced composite material for which material properties are specified with respective to a material axis aligned with layer fibre orientation (i.e. co-ordinates X_1, X_2, X_3 where X_1 corresponds to the fibre direction, X_2 is the in-plane co-ordinate perpendicular to X_1, and X_3 is the transverse co-ordinate which is parallel to the global co-ordinate z, as shown in Fig. 3.2). The required S^i matrix relates stresses and strains in the global co-ordinate system (x, y, z). The material and global co-ordinates are related by an in-plane rotation, θ, where θ is the angle (measured positive counter clockwise) from the global axis x to the fibre direction X_1. Applying transformation laws

and assuming the ordering of layer stresses is $\underline{\sigma}^{i^T} = \left[\sigma_x^i \ \sigma_y^i \ \sigma_z^i \ \sigma_{yz}^i \ \sigma_{xz}^i \ \sigma_{xy}^i\right]$, S^i is in the form

$$S^i = \begin{bmatrix} S_{11} & S_{12} & S_{13} & 0 & 0 & S_{16} \\ S_{12} & S_{22} & S_{23} & 0 & 0 & S_{26} \\ S_{13} & S_{23} & S_{33} & 0 & 0 & S_{36} \\ 0 & 0 & 0 & S_{44} & S_{45} & 0 \\ 0 & 0 & 0 & S_{45} & S_{55} & 0 \\ S_{16} & S_{26} & S_{36} & 0 & 0 & S_{66} \end{bmatrix}$$

where, with $m = \cos\theta$ and $n = \sin\theta$

$$S_{11} = \frac{m^4}{E_{11}} + \frac{n^4}{E_{22}} + m^2n^2\left[\frac{1}{G_{12}} - 2\frac{\nu_{12}}{E_{11}}\right]$$

$$S_{12} = m^2n^2\left[\frac{1}{E_{11}} + \frac{1}{E_{22}} - \frac{1}{G_{12}}\right] - (m^4 + n^4)\frac{\nu_{12}}{E_{11}}$$

$$S_{13} = -\left[m^2\frac{\nu_{12}}{E_{11}} + n^2\frac{\nu_{23}}{E_{22}}\right]$$

$$S_{16} = 2mn\left[\frac{m^2}{E_{11}} - \frac{n^2}{E_{22}}\right] - mn(m^2 - n^2)\left[\frac{1}{G_{12}} - \frac{\nu_{12}}{E_{11}}\right]$$

$$S_{22} = \frac{n^4}{E_{11}} + \frac{m^4}{E_{22}} + m^2n^2\left[\frac{1}{G_{12}} - 2\frac{\nu_{12}}{E_{11}}\right]$$

$$S_{23} = -\left[n^2\frac{\nu_{12}}{E_{11}} + m^2\frac{\nu_{23}}{E_{22}}\right] \qquad (2)$$

$$S_{26} = 2mn\left[\frac{n^2}{E_{11}} - \frac{m^2}{E_{22}}\right] + mn(m^2 - n^2)\left[\frac{1}{G_{12}} - 2\frac{\nu_{12}}{E_{11}}\right]$$

$$S_{33} = \frac{1}{E_{22}}$$

$$S_{36} = 2mn \left[\frac{\nu_{23}}{E_{22}} - \frac{\nu_{12}}{E_{11}} \right]$$

$$S_{44} = \frac{m^2}{G_{23}} + \frac{n^2}{G_{12}}$$

$$S_{45} = mn \left[\frac{1}{G_{12}} - \frac{1}{G_{23}} \right]$$

$$S_{55} = \frac{n^2}{G_{23}} + \frac{m^2}{G_{12}}$$

$$S_{66} = 4m^2n^2 \left[\frac{1}{E_{11}} + \frac{1}{E_{22}} + 2\frac{\nu_{12}}{E_{11}} \right] + (m^2 - n^2)^2 \frac{1}{G_{12}}$$

In equation (2), E_{11} and E_{22} are Young's moduli in the fibre and transverse direction, respectively, ν_{12} and ν_{23} are the major and minor Poisson's ratios.

Returning now to the element formulation based on Eq. (1), stresses in the layer are assumed in terms of a finite set of stress parameters, $\underline{\beta}^i$, for layer i, in the form

$$\underline{\sigma}^i = P^i \underline{\beta}^i \qquad (3)$$

where P^i consists of polynomial terms and is defined so that the homogeneous equilibrium equations are exactly satisfied. The typical set of polynomials used for present analysis are given in the Appendix-A.

An isoparametric transformation is assumed in the present element which relates the x and y to in-plane normalized coordinates (ξ, η) (an 8-node mapping for present element

$$x = \sum_{j=1}^{8} N_j(\xi,\eta)\ x_j \tag{4a}$$

$$y = \sum_{j=1}^{8} N_j(\xi,\eta)\ y_j \tag{4b}$$

where $N_j(\xi,\eta)$ corresponds to the biquadratic Serendipity shape functions (given in the Appendix-B) and (x_j,y_j) are the global in-plane co-ordinates of node j. In addition, a normalized transverse co-ordinate, ζ, is introduced for each layer which is related to z by

$$z = \frac{1}{2}\left[(h_i + h_{i+1}) + \zeta(h_{i+1} - h_i)\right] \tag{5}$$

so that $\zeta = -1$ at the bottom of the layer i and $\zeta = +1$ at the top of the layer i. Using Eqs. (4) and (5), P^i (which is typically expressed in the x,y,z co-ordinates) can be expressed in terms of normalized co-ordinates (ξ,η,ζ).

The displacements $\underline{u}^i$ for layer i are interpolated in terms of nodal displacements, $\underline{q}^i$, for layer i in the form of

$$\underline{u}^i = N^i\ \underline{q}^i \tag{6}$$

where N^i are the shape functions expressed in the normalized co-ordinates (ξ,η,ζ). By applying the linear strain-displacement relations to Eq. (6), $\hat{\underline{\varepsilon}}^i$ can be related to $\underline{q}^i$ as

$$\hat{\underline{\varepsilon}}^i = D^i\ \underline{u}^i = D^i\ N^i\ \underline{q}^i = B^i\ \underline{q}^i = \frac{1}{|J|}\ B^{*i}\ \underline{q}^i \tag{7}$$

where D^i is the strain-displacement differential operator matrix, and $|J|$ is the Jacobian of the transformation given by the Eqs. (4). Assuming that $\underline{u}^i$ is the ordered $\underline{u}^{iT} = [u\ v\ w]^i$ (displacements in the x,y and z directions respectively) and that components of $\hat{\underline{\varepsilon}}^i$ are ordered as previously described for $\underline{\sigma}^i$, D^i is given by

$$D^i = \frac{1}{|J|}\begin{bmatrix} \left(\frac{\partial y}{\partial \eta}\frac{\partial}{\partial \xi} - \frac{\partial y}{\partial \xi}\frac{\partial}{\partial \eta}\right) & \emptyset & \emptyset \\ \emptyset & \left(\frac{\partial x}{\partial \xi}\frac{\partial}{\partial \eta} - \frac{\partial x}{\partial \eta}\frac{\partial}{\partial \xi}\right) & \emptyset \\ \emptyset & \emptyset & \frac{|J|}{\bar{t}_i}\frac{\partial}{\partial \zeta} \\ \emptyset & \frac{|J|}{\bar{t}_i}\frac{\partial}{\partial \zeta} & \left(\frac{\partial x}{\partial \xi}\frac{\partial}{\partial \eta} - \frac{\partial x}{\partial \eta}\frac{\partial}{\partial \xi}\right) \\ \frac{|J|}{\bar{t}_i}\frac{\partial}{\partial \zeta} & \emptyset & \left(\frac{\partial y}{\partial \eta}\frac{\partial}{\partial \xi} - \frac{\partial y}{\partial \xi}\frac{\partial}{\partial \eta}\right) \\ \left(\frac{\partial x}{\partial \xi}\frac{\partial}{\partial \eta} - \frac{\partial x}{\partial \eta}\frac{\partial}{\partial \xi}\right) & \left(\frac{\partial y}{\partial \eta}\frac{\partial}{\partial \xi} - \frac{\partial y}{\partial \xi}\frac{\partial}{\partial \eta}\right) & \emptyset \end{bmatrix}$$

where the transformation of Eq. (4) is used in Eq. (8) and $\bar{t}_i$ is half the thickness of layer i, i.e.

$$\bar{t}_i = \left(\frac{h_{i+1} - h_i}{2}\right) \tag{9}$$

Eqs. (3), (6) and (7) are substituted into Eq. (1) and following layer matrices are defined:

$$H^i = \bar{t}_i \int_{-1}^{1}\int_{-1}^{1}\int_{-1}^{1} P^{i^T} S^i P^i |J| \, d\xi \, d\eta \, d\zeta \tag{10a}$$

$$G^i = \bar{t}_i \int_{-1}^{1}\int_{-1}^{1}\int_{-1}^{1} P^{i^T} B^{*^i} \, d\xi \, d\eta \, d\zeta \tag{10b}$$

$$Q^i = \int_{S_{\sigma_{n_i}}} N^{i^T} \bar{T}^i \, ds \tag{10c}$$

so that π becomes

$$\pi_{mc} = \sum_n \sum_I \left\{ \frac{1}{2} \beta^{i^T} H^i \beta^i - \beta^{i^T} G^i q^i + q^{i^T} Q^i \right\} \tag{11}$$

At this stage, stresses and displacements are independent from layer to layer. However enforcement of traction continuity along inter-layer surfaces will require that certain of the β^{i+1} be related to certain of the β^i (i.e. inter face between layers

i and i+1). As a result of such relations, a final set of linearly independent stress parameters, $\underline{\beta}$, can be defined for the laminate. Similarly certain of nodal displacements, q^{i+1}, will be related to certain of q^{i} in order to satisfy displacement continuity along the interlayer surface between layers i and i+1, and a final set of linearly independent nodal displacements, $\mathbf{q}$, can be defined for the laminate.

Corresponding to these interlayer surface continuity conditions, layer stress parameters, β^{i}, and nodal displacements, q^{i}, can be related to the laminate stress parameters, $\underline{\beta}$, and nodal displacements, $\mathbf{q}$, respectively, in the form;

$$\underline{\beta}^{i} = C_{s}^{i}\,\underline{\beta} \tag{12a}$$

$$\mathbf{q}^{i} = C_{d}^{i}\,\mathbf{q} \tag{12b}$$

By substituting above equations into Eq.(11), π_{mc} is now expressed in terms of laminate/element stress and displacement parameters. Therefore, the summation over the layers can be taken inside and the following laminate matrices defined:

$$\mathbf{H} = \sum_{i} C_{s}^{i\,T} H^{i} C_{s}^{i} \tag{13a}$$

$$\mathbf{G} = \sum_{i} C_{s}^{i\,T} G^{i} C_{d}^{i} \tag{13b}$$

$$\mathbf{Q} = \sum_{i} C_{d}^{i\,T} Q^{i} \tag{13c}$$

In the above equations matrix multiplications are not carried out explicitly. The operations in the above equations are similar to element 'assembly' operations; a set of layer-to-laminate parameters 'pointers' and nodal displacement 'pointers' can be used to locate layer matrix contributions in the

With the definition of Eq. (1), π becomes

$$\pi_{mc} = \sum_{n} \left\{ -\frac{1}{2}\underline{\beta}^T H \underline{\beta} - \underline{\beta}^T G \underline{q} + \underline{q}^T Q \right\} \tag{14}$$

which is now the standard form of hybrid stress elements.

The variation of functional π_{mc} with respect to β yields

$$\frac{\partial \pi_{mc}}{\partial \beta} = \emptyset$$

or $$H\underline{\beta} - G\underline{q} = \emptyset$$

or $$\underline{\beta} = H^{-1} G \underline{q} \tag{15}$$

and $$\frac{\partial \pi_{mc}}{\partial q} = \emptyset$$

or $$G^T \underline{\beta} = Q$$

$$G^T H^{-1} G \underline{q} = Q \tag{16}$$

Therefore elemental stiffness matrix is given by

$$K = G^T H^{-1} G \tag{17}$$

and Q is the elemental load vector.

Once nodal displacements have been calculated, stresses for each layer are calculated by obtaining $\underline{\beta}$ from Eq. (15), $\underline{\beta}^i$ from Eq. (12a) (by extracting the appropriate $\underline{\beta}^i$ from $\underline{\beta}$), and substituting into Eq. (3). Strains $\underline{\varepsilon}^i$ can be obtained from stresses $\underline{\sigma}^i$ by using S^i.

3.3 DISPLACEMENT AND STRESS INTERPOLATION FOR A LAYER

3.3.1 Displacement Interpolation

All components of displacements are included since

bending/stretching coupling will exit, independent of plate thickness, for any unbalanced fibre-reinforced laminate. Moderately thick and thick laminates is characterized by severe cross-sectional warping, and each layer must be allowed to undergo independent non-normal cross-section rotations, while preserving interlayer surface displacement continuity.

To incorporate this warping behavior, all displacement components (u, v and w in x, y and z directions, respectively) are assumed to vary linearly, through the thickness of each layer. The degrees of freedom at element spanwise node j, which guarantee interlayer surface displacement continuity, are therefore u_j^i, v_j^i and w_j^i at the bottom, each interlayer, upper surface (i = 1,2,3...I+1) (Fig. 3.3). The displacement interpolations in normalized co-ordinates for typical layer i are then given as

$$u^i(\xi,\eta,\zeta) = \sum_{j=1}^{8} N_j(\xi,\eta)\left[-\frac{1}{2}(1-\zeta)u_j^i + \frac{1}{2}(1+\zeta)u_j^{i+1}\right] \quad (18a)$$

$$v^i(\xi,\eta,\zeta) = \sum_{j=1}^{8} N_j(\xi,\eta)\left[-\frac{1}{2}(1-\zeta)v_j^i + \frac{1}{2}(1+\zeta)v_j^{i+1}\right] \quad (18b)$$

$$w^i(\xi,\eta,\zeta) = \sum_{j=1}^{8} N_j(\xi,\eta)\left[-\frac{1}{2}(1-\zeta)w_j^i + \frac{1}{2}(1+\zeta)w_j^{i+1}\right] \quad (18c)$$

where $N_j(\xi,\eta)$ are the standard 8-node biquadratic Serendipity shape functions (shown in Appendix-B).

The u_j^i, u_j^{i+1}, v_j^i, v_j^{i+1}, w_j^i, w_j^{i+1} are treated as layer degrees of freedom, $\underline{q}^i$; Eqs. (18) then define N^i of Eq. (6), from which B^{*i} of Eq. (7) can be computed. With an assumed ordering of laminate degrees of freedom,

$$q^T = \left[u_1^1 u_1^2 \ldots u_1^{I+1} v_1^1 v_1^2 \ldots v_1^{I+1} w_1^1 w_1^2 \ldots w_1^{I+1} u_2^1 u_2^2 \ldots u_2^{I+1} v_2^1 v_2^2 \ldots v_2^{I+1} w_2^1 w_2^2 \ldots\right.$$

the Boolean matrix C_d^i of Eq. (12b) can be defined. For I layers, the 8-node element based on the 'general' displacement field of Eqs. (18) will have 24(I + 1) total degrees of freedom per element and 3(I + 1) degrees of freedom per node.

3.3.2 Layer Stress Interpolation

All components of stresses are included and are interpolated within each layer in terms of stress parameters, $\underline{\beta}^i$, for that layer, such that homogeneous equilibrium equations are exactly satisfied. Introducing the normalized transverse layer co-ordinate, ζ, these equations are

$$\frac{\partial \sigma_x^i}{\partial x} + \frac{\partial \sigma_{xy}^i}{\partial y} + \frac{1}{t_i}\frac{\partial \sigma_{xz}^i}{\partial \zeta} = \emptyset \qquad (20a)$$

$$\frac{\partial \sigma_{xy}^i}{\partial x} + \frac{\partial \sigma_y^i}{\partial y} + \frac{1}{t_i}\frac{\partial \sigma_{yz}^i}{\partial \zeta} = \emptyset \qquad (20b)$$

$$\frac{\partial \sigma_{xz}^i}{\partial x} + \frac{\partial \sigma_{yz}^i}{\partial y} + \frac{1}{t_i}\frac{\partial \sigma_z^i}{\partial \zeta} = \emptyset \qquad (20c)$$

The stresses $\sigma_x^i(x,y,\zeta)$, $\sigma_y^i(x,y,\zeta)$ and $\sigma_{xy}^i(x,y,\zeta)$ are assumed to vary linearly in ζ within the layer; from Eqs. (20a)and (20b), $\sigma_{xz}^i(x,y,\zeta)$ and $\sigma_{yz}^i(x,y,\zeta)$ must be of order ζ^2, from Eq. (20c) $\sigma_z^i(x,y,\zeta)$ must be of order ζ^3 within the layer. A 67β, generalized hybrid stress assumption used in the present analysis is presented in Appendix-A. It may be noted that the stretching portions of σ_x^i, σ_y^i and σ_{xy}^i remain complete cubic polynomials in x, y, σ_{xz}^i and σ_{yz}^i include all quadratic x, y terms and σ_z^i is linear in x, y.

The alternative layer stress fields satisfy the

parameters are independent from layer to layer. In the present element used, the interlayer traction continuity are satisfied by establishing a set of element/laminate stress parameters, β, and relating layer β^i to β as in Eq. (12a).

The interlayer surface traction continuity requires that σ_{xz}, σ_{yz} and σ_z be continuous at interlayer surfaces. For example for the polynomials assumed in present analysis (Appendix-A), evaluation of these stresses at lower surface ($\zeta = -1$) of layer i yields :

$$\sigma^i_{xz}\Big|_{\zeta=-1} = \bar{t}_i(\beta^i_1 + \beta^i_2 x + \beta^i_3 y + \beta^i_4 x^2 + \beta^i_5 xy + \beta^i_6 y^2)$$

$$\sigma^i_{yz}\Big|_{\zeta=-1} = \bar{t}_i(\beta^i_7 + \beta^i_8 x + \beta^i_9 y + \beta^i_{10} x^2 + \beta^i_{11} xy + \beta^i_{12} y^2) \qquad (21)$$

$$\sigma^i_{z}\Big|_{\zeta=-1} = \bar{t}^2_i(\beta^i_{13} + \beta^i_{14} x + \beta^i_{15} y)$$

and the upper surface ($\zeta = +1$) of layer i;

$$\sigma^i_{xz}\Big|_{\zeta=1} = \bar{t}_i(\beta^i_{53} + \beta^i_{54} x + \beta^i_{55} y + \beta^i_{56} x^2 + \beta^i_{57} xy + \beta^i_{58} y^2)$$

$$\sigma^i_{yz}\Big|_{\zeta=1} = \bar{t}_i(\beta^i_{59} + \beta^i_{60} x + \beta^i_{61} y + \beta^i_{62} x^2 + \beta^i_{63} xy + \beta^i_{64} y^2) \qquad (22)$$

$$\sigma^i_{z}\Big|_{\zeta=1} = \bar{t}^2_i(\beta^i_{65} + \beta^i_{66} x + \beta^i_{67} y)$$

With the simple form of transverse shear and normal stresses at interlayer surfaces, the traction continuity condition at the interface between layers $i-1$ and i (where $i > 1$) requires that

$$\beta^i_j = \frac{\bar{t}_{i-1}}{\bar{t}_i}\beta^{i-1}_{j+52} \qquad j = 1,2,\ldots 12 \qquad (23a)$$

$$\frac{\bar{t}^2_{i-1}}{}$$

thus the set of independent laminate stress parameters, β, for present element is reduced to

$$\underline{\beta}^T = \left[\beta_1^1 \beta_2^1 \ldots \beta_{\sigma 7}^1 \beta_{16}^2 \beta_{17}^2 \ldots \beta_{\sigma 7}^2 \ldots \beta_{16}^I \beta_{17}^I \ldots \beta_{\sigma 7}^I \right] \qquad (24)$$

Thus the total number of independent stress parameters for I layer laminate is (67 - 15)I.

The C_s^i of Eq.(12b) can be constructed for each layer using Eq. (23) and the laminate $\underline{\beta}$ of Eq.(24). In practice, matrix multiplications in Eq. (13a) and Eq. (13b) involving C_s^i are not performed. Instead, row and column in H^i and rows in G^i corresponding to $\beta_1^i - \beta_{15}^i$ are scale per Eqs. (23), after which a set of layer-to-laminate stress parameter 'pointers' are used to appropriately assemble the scaled H^i into H and G into G^i.

3.4 PROGRAM CHARACTERISTICS

A program has been developed based on above formulation, the block diagram of which is as shown in Fig. 3.4.

While developing the program attempt has been made to modularise the entire calculations in subroutines so that following objectives are fulfilled to the highest possible extent.

i)Repetition of calculations is avoided. This is very important to the efficiency of program.

ii)Program build up is easy and each module could be separately tested and assembled into the whole program.

It is important to mention here that Frontal solving technique for solving final simultaneous equations is employed in the present work. The main advantage of Frontal technique is that, it requires less in-core memory.

midside nodes if they lie in a straight edge there by avoiding entry of co-ordinates of all nodes manually.

With the P^i matrix (Eq.(3)) defined using the appropriate stress field and B^{*i} (Eq. (7)) defined as described earlier, the layer matrices H^i (Eq. (1Øa)) and G^i (Eq. (1Øb)) can be computed using numerical integration; here 4x4x4 Gauss rule is used.

In present element, the optimal sampling points for stress evaluation are at the 2x2 Gauss station in x-y plane.

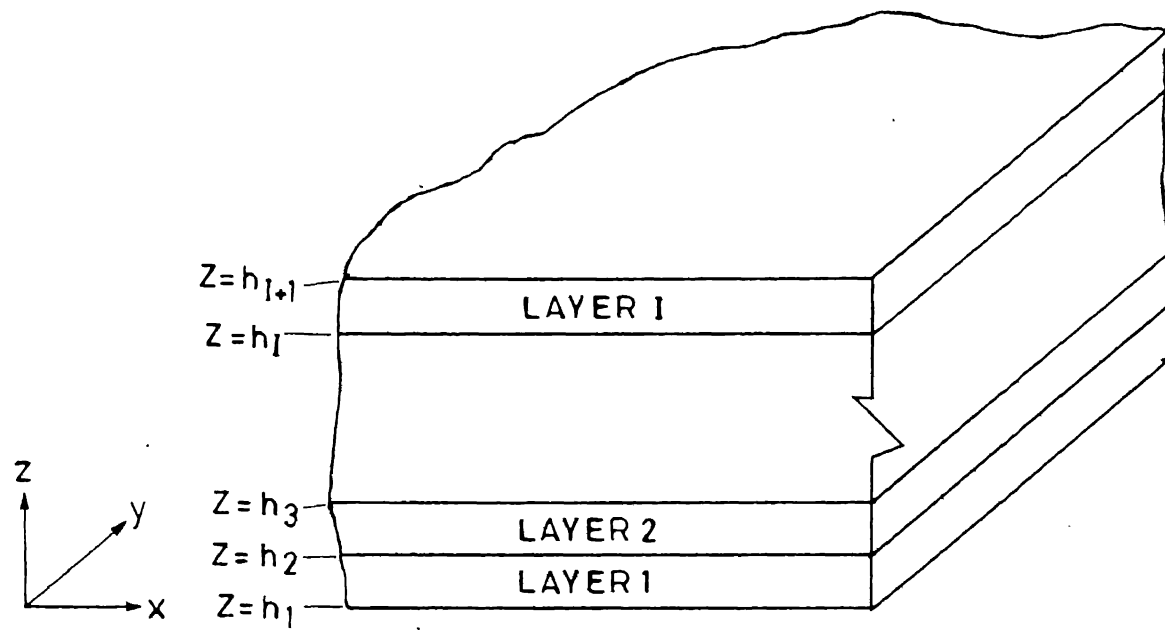

FIG. 3.1 GEOMETRY AND LAYER NUMBERING OF MULTILAYER PLATE ELEMENT

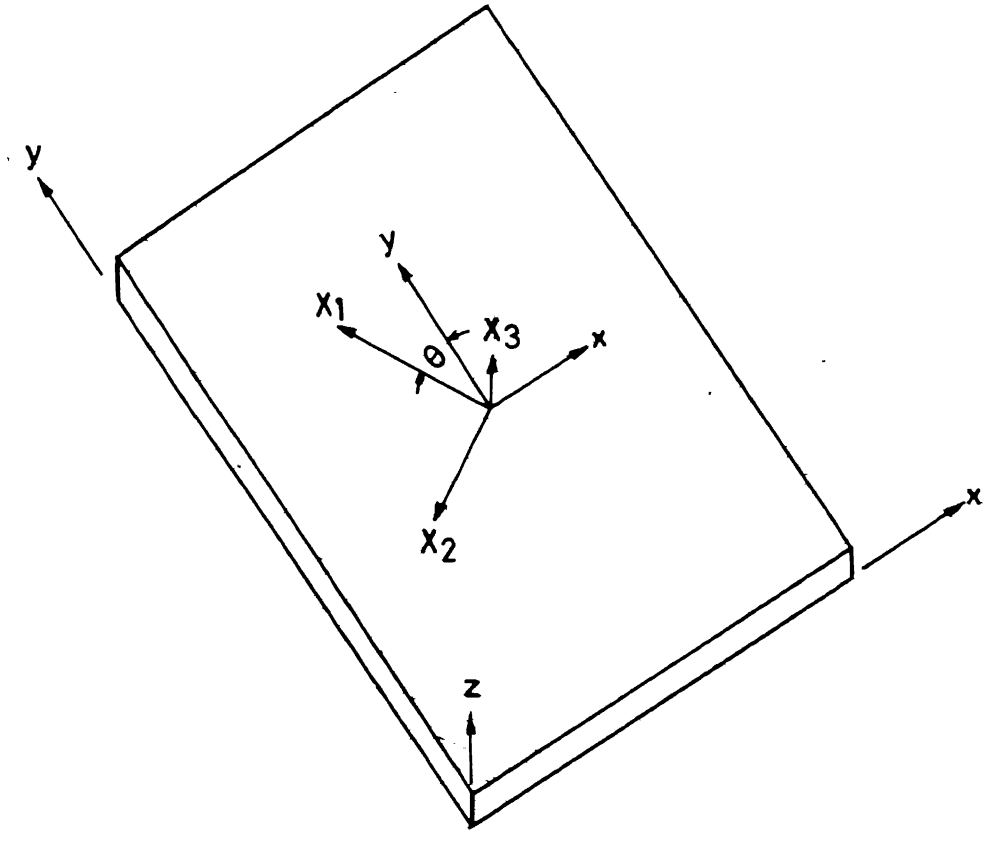

FIG. 3.2 LAMINA WITH ITS PRINCIPAL MATERIAL AXES ORIENTED AT ANGLE θ WITH REFERENCE TO GLOBAL COORDINATE AXES

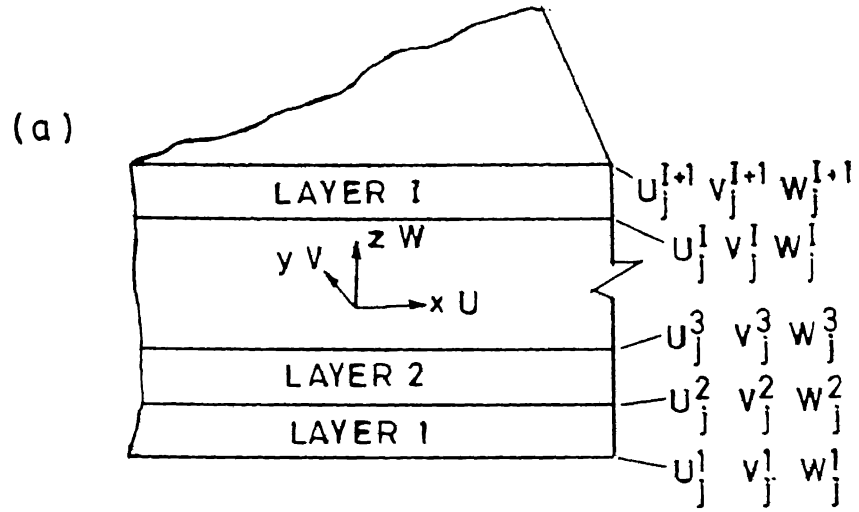

DISPLACEMENT DEGREE OF FREEDOM AT NODE j OF THE LAMINATE

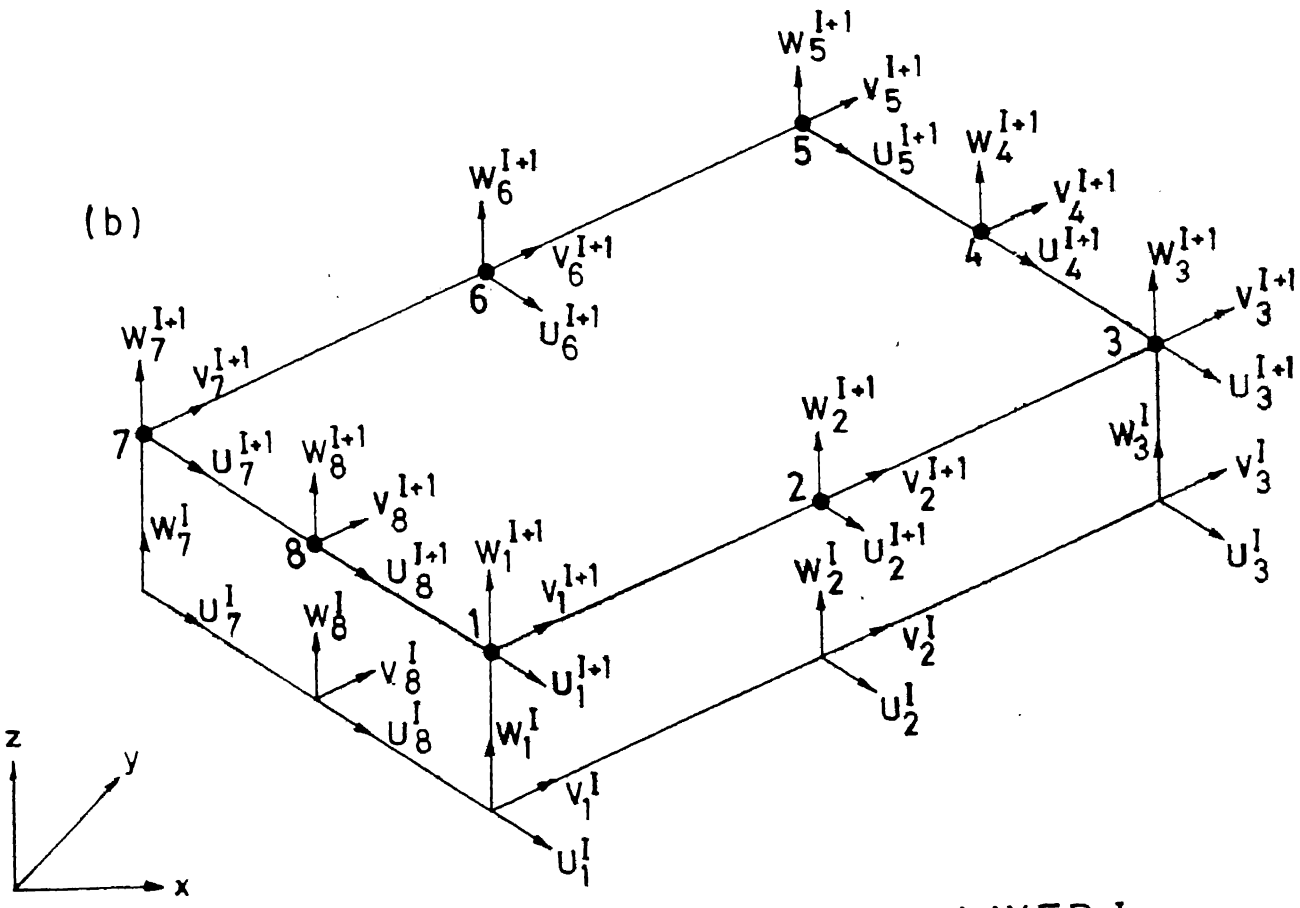

DISPLACEMENT DEGREES OF FREEDOM FOR LAYER I

FIG.3-3 DISPLACEMENT DEGREES OF FREEDOM

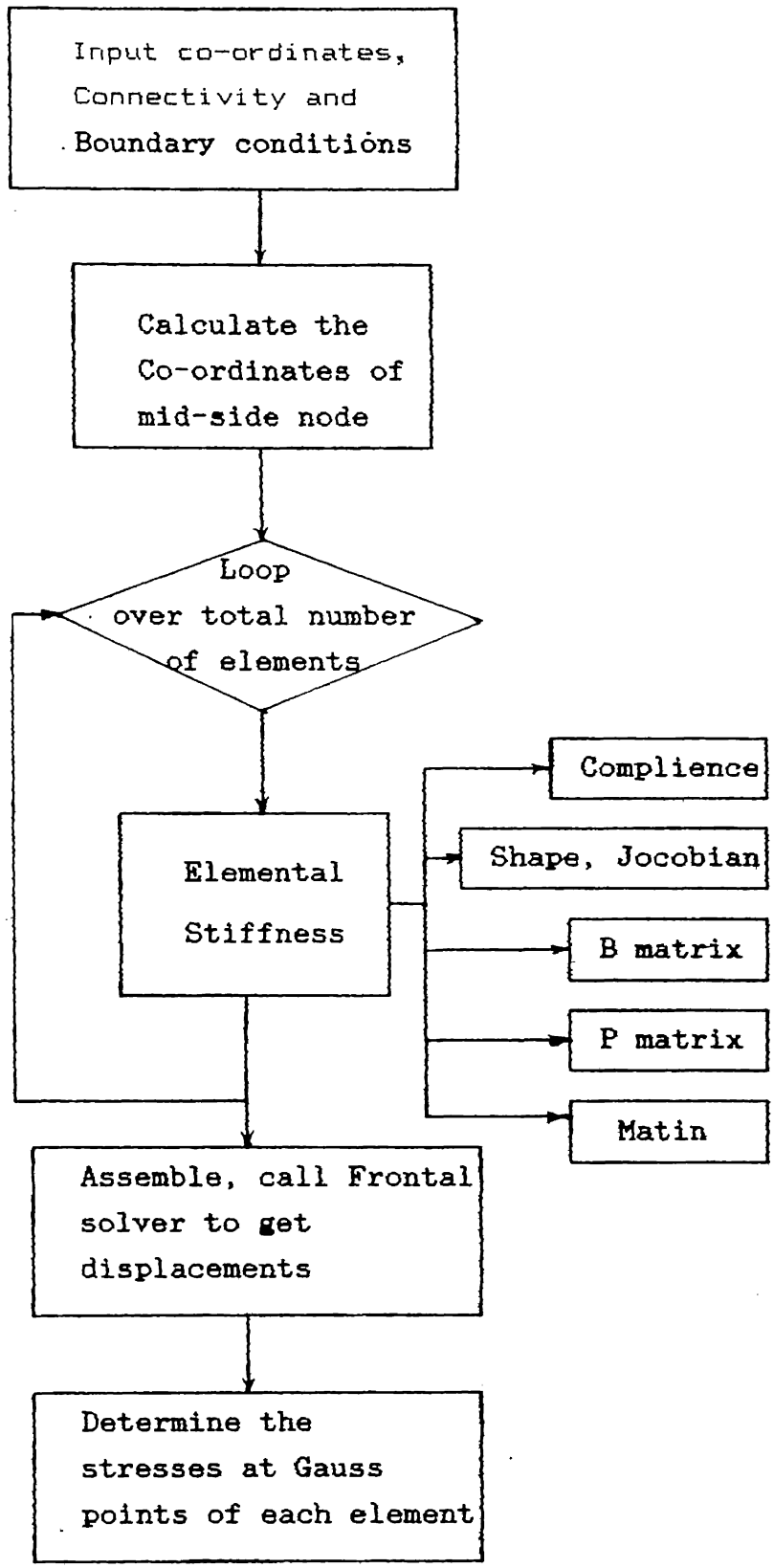

Fig. 3.4 Program Structure

CHAPTER IV

RESULTS AND DISCUSSIONS

This chapter presents the free-edge stresses in laminated composites plates subjected to far field uniform strain ε_y by the hybrid finite element method. Three geometries have been considered for analysis:

1) a simple symmetric composite plate
2) a symmetric composite plate with circular hole
3) a symmetric composite plate with square hole

4.1 EDGE-STRESSES IN A COMPOSITE PLATE

In this analysis symmetric laminate of $[0/90]_s$, $[90/0]_s$, $[-45/+45]_s$ and $[+45/-45]_s$ configurations have been considered. The material properties of plies used are as mentioned in chapter-II. Fig 4.1 shows the geometry of plate and two finite element discretization. It may be noted that the nature of the load and geometry and material properties of the plate, are such that the edge stresses are identical at any cross-section perpendicular to y-axis and thus it is sufficient to consider one strip of elements at any cross-section (xy - plane). It is also shown in figure two types of meshes: one with 10 elements and other with 15 elements.

Fig 4.2 shows the variation of interlaminar normal stress, σ_z at ply interface of 0^o and 90^o layers of $[0/90]_s$ laminate. The stresses at interface of 0^o and 90^o layers are

determined by taking average of stress values at the Gauss points just above and below the interface. The distance from free edge is normalized with respective to the total laminate thickness. As can be seen that the difference between the present results and those obtained by Pagano (1974) is around 10% near the edge. Fig 4.3 presents the results of hybrid finite element with 15 elements mesh. Here also the results of Pagano (1974) have been presented for comparison. It may be noted that the results using this finer mesh and those of earlier mesh are almost same, excepting that the stress values very near the edge are approximated better.

Thus, it is concluded that a mesh with 15 elements gives sufficiently converged results and hence such mesh is used for all configurations. Fig. 4.4 shows the interlaminar normal stress, σ_z at the ply interface of 0° and 90° layers of $[90/0]_s$ laminate. These are compared with those of Spilker and Chou (1980) and they are in good agreement.

The edge stress σ_z in case of $[+45/-45]_s$ configuration are shown in Fig 4.5 and those in $[-45/+45]_s$ are shown in Fig 4.6. It may be observed that the edge-stress, σ_z, values are compressive and almost same in both these configurations except at very much near the edge.

The hybrid analysis has been modified to take into account the traction free nature of the free edge [Spilker (1982)]. This required that 23 β's to be made zero for the element bordering the edge so that the stress components σ_x, σ_{xy} and σ_{xz} becomes zero on the free edge. The interlaminar normal stress σ_z in case of 10 elements discretization is as shown in Fig 4.7. The

figure also includes the plot of σ_z with same mesh discretization but without this conditions. It may be observed that the difference in the stress values is negligible every where except near the edge and also the variation has become less smooth. Thus, it is felt that such imposition of traction free condition on the edge may not be necessary.

4.2 INTERLAMINAR STRESSES NEAR THE CIRCULAR HOLE BOUNDARY IN SYMMETRIC COMPOSITE LAMINATE

As discussed in chapter-I, there are situations where the composite laminate have holes, cut outs etc., which is possible site for delamination. The interlaminar stresses near the free edge of a circular hole in symmetric laminate $[\emptyset/90]_s$ have been investigated. The material properties of the plies are assumed to be same as given in chapter-II . Fig. 4.8 shows the finite element discretization of a laminated composite with circular hole. The laminate is subjected to a uniform far field strain in y-direction. As may be observed that one eighth of the plate is modelled in the analysis due to the symmetries of the problem about x, y and z axes. The mesh is fine near the hole boundary and has a total of 27 elements. The hybrid finite analysis has also been performed with finer mesh having a total of 70 elements as shown in Fig. 4.9.

The interlaminar stress σ_z between 0° and 90° layers, variation is shown in Fig. 4.10. The variations are plotted along radial lines at angles 0°, 45°, 90° with respective the far field loading direction (i.e. y-axis). In the figure stress σ_z is

normalized with a factor S_g as given by

$$S_g = 3Ø2\ u_o/h \quad \text{Mpa}$$

$$S_g = 43x1Ø^3\ u_o/h \quad \text{Psi}$$

where S_g represents gross section stress necessary for this deformation. As can be seen the interlaminar stress variations are qualitatively same in the analyses by the two meshes, the variation being smooth in the case of the finer mesh. In the Fig. 4.1Ø the results obtained by Raju and Crews (1982) are plotted. Their analyses was by 8-noded brick elements using very fine mesh. It can be observed the variation is same qualitatively in $\theta = 9Ø^\circ$ case. In the case of variation along $\theta = Ø^\circ$ line the present analysis shows very negligible interlaminar normal stress σ_z as is expected. Along $\theta = 45^\circ$ line there is some discrepancy and there are no other results available for comparison in the literature for the present problem. It's worth noting that the interlaminar normal stress σ_z is tensile near the edge near $\theta = 45^\circ$ and $\theta = 9Ø^\circ$ indicating that it is a possible location for delamination initiation and growth.

Figs. 4.11 and 4.12 shows the interlaminar shear stress, σ_{xz} and σ_{yz} variation near the hole boundary along the radial lines $\theta = Ø^\circ$, $\theta = 45^\circ$ and $\theta = 9Ø^\circ$. One feature worth noting is that the shear stresses along $\theta = 9Ø^\circ$ and $\theta = 45^\circ$ are significant over a larger length and in conjugation with normal stress may lead to mixed mode fracture.

Normal stress, σ_z very near the free edge of the circular hole variation in the thickness direction is presented in Fig. 4.13. Here the thickness direction is plotted along y-axis and the normalized stress along the x-axis. It may be seen that at θ

= 0° the normal stress anywhere in the thickness is more or less zero and at $\theta = 90^{\circ}$ is tensile at the interface and in the top layer, (i.e., 0° layer) whereas the normal stress is tensile in the both the layers and significant at $\theta = 45^{\circ}$.

4.3 EDGE STRESSES NEAR THE SQUARE HOLE BOUNDARY IN SYMMETRIC COMPOSITE LAMINATE

Similar to the analysis of edge stresses near a circular hole in a symmetric laminate, hybrid finite element method analysis is carried out in the case of a $[0/90]_s$ laminate with a square hole. The laminate geometry and material properties are assumed to be same as in the previous case. The finite element discretization of the laminate is shown in Fig. 4.14. The mesh is made finer near the hole and has a total number of 45 elements. The stresses at the interface of 0° and 90° layers is computed as explained in section 4.2.

The interlaminar normal stress, σ_z is shown in Fig. 4.15. The three curves represent the stress variation along the radial lines $\theta = 0^{\circ}$, $\theta = 45^{\circ}$ and $\theta = 90^{\circ}$. Here also, the normal stress at $\theta = 0^{\circ}$ is negligible whereas it has significant positive value near $\theta = 45^{\circ}$ and $\theta = 90^{\circ}$. These values seem to be more than those in the case of circular hole. However, overall the variation is same. Thus square hole seems to have more tendency for delamination.

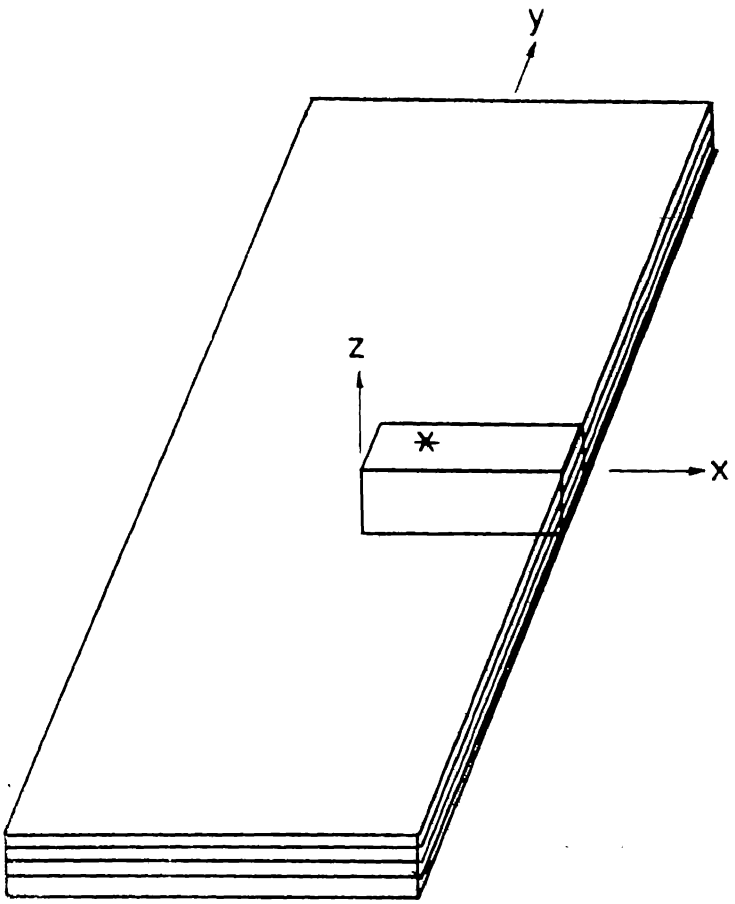

	Mesh (i)	Mesh (ii)
No. of elements	= 10	15
No. of nodes	= 53	78
Total degrees of freedom	= 477	702
b	= 12"	12"
Ply thickness	= 0.75"	0.75"

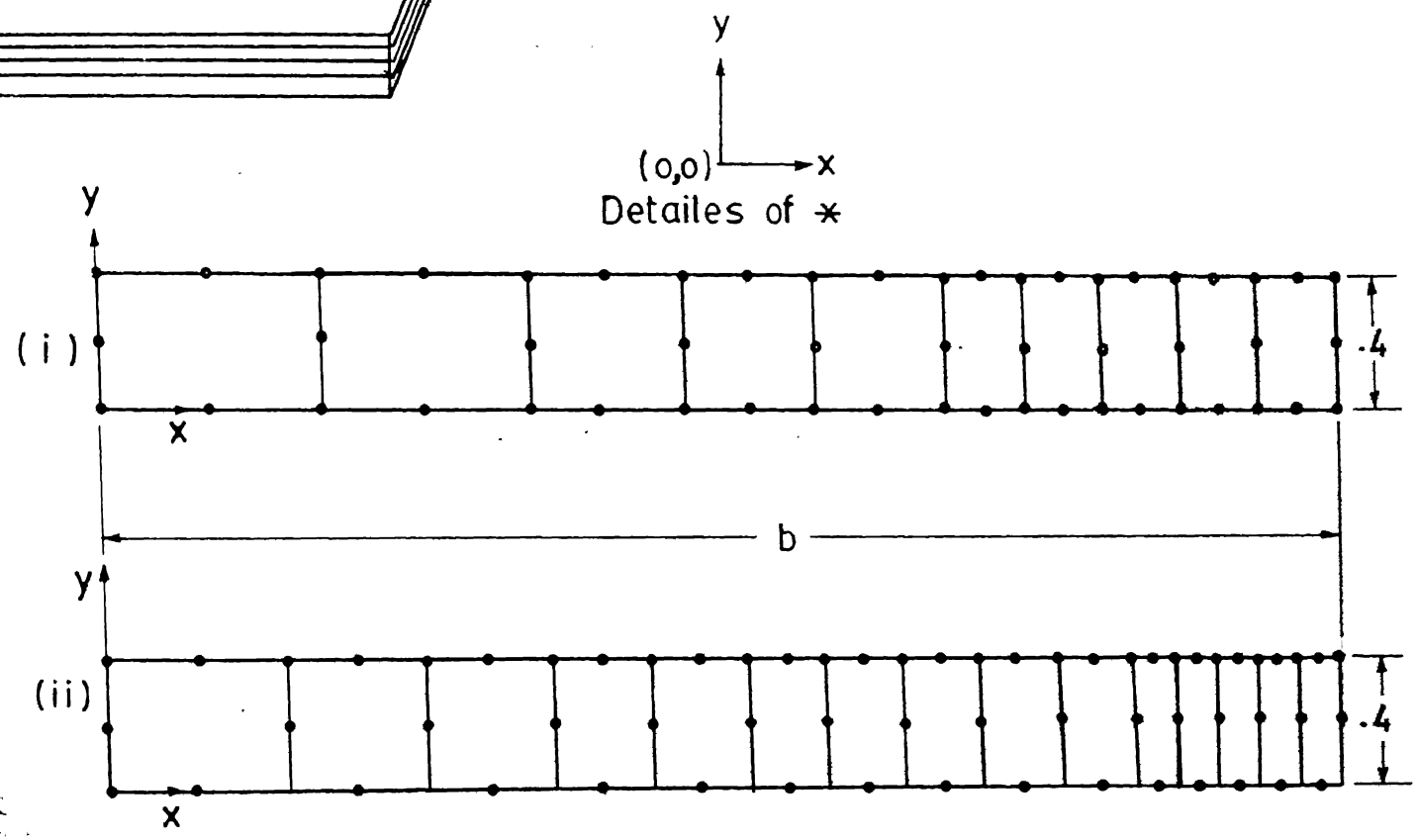

FIG 4.1 FEM IDEALIZATION OF LAMINATED PLATE

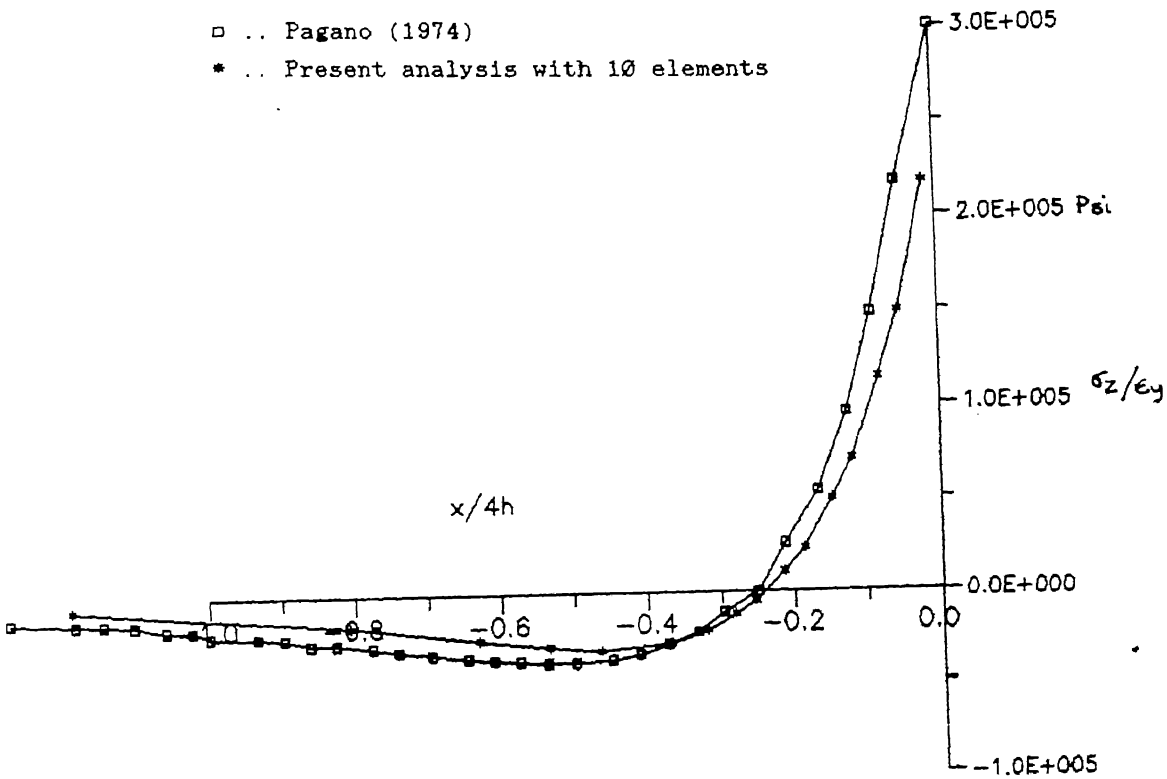

Fig.4.2 Distribution of σ_z of $[0/90]_s$ laminated plate at ply interface

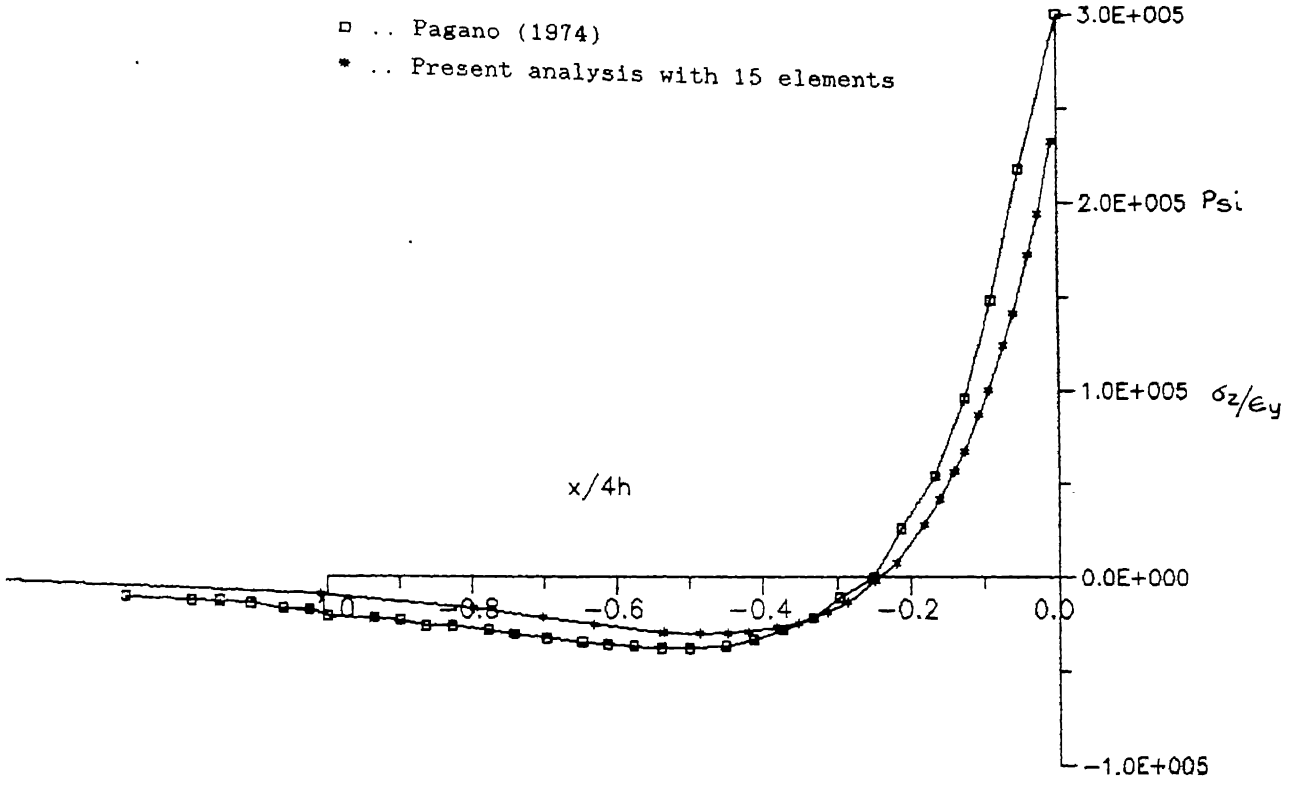

Fig.4.3 Distribution of σ_z of $[0/90]_s$ laminated plate at ply interface

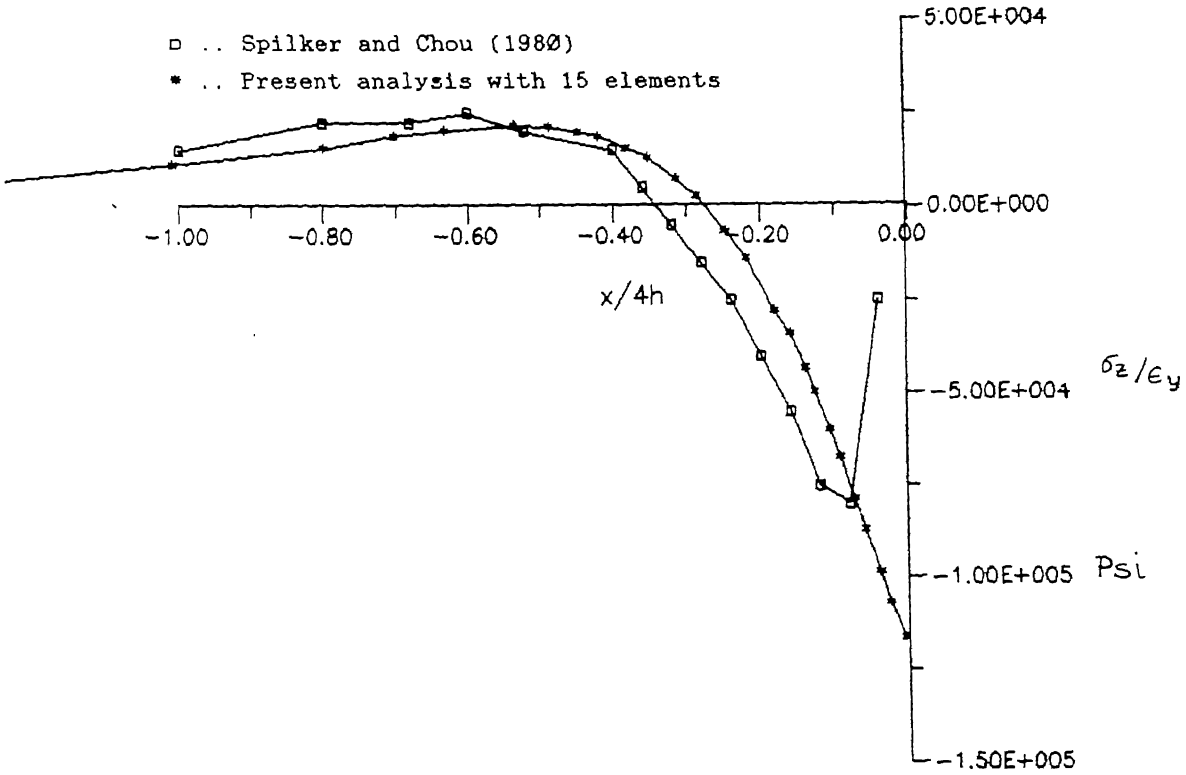

Fig.4.4 Distribution of σ_z of $[90/0]_s$ laminated plate at ply interface

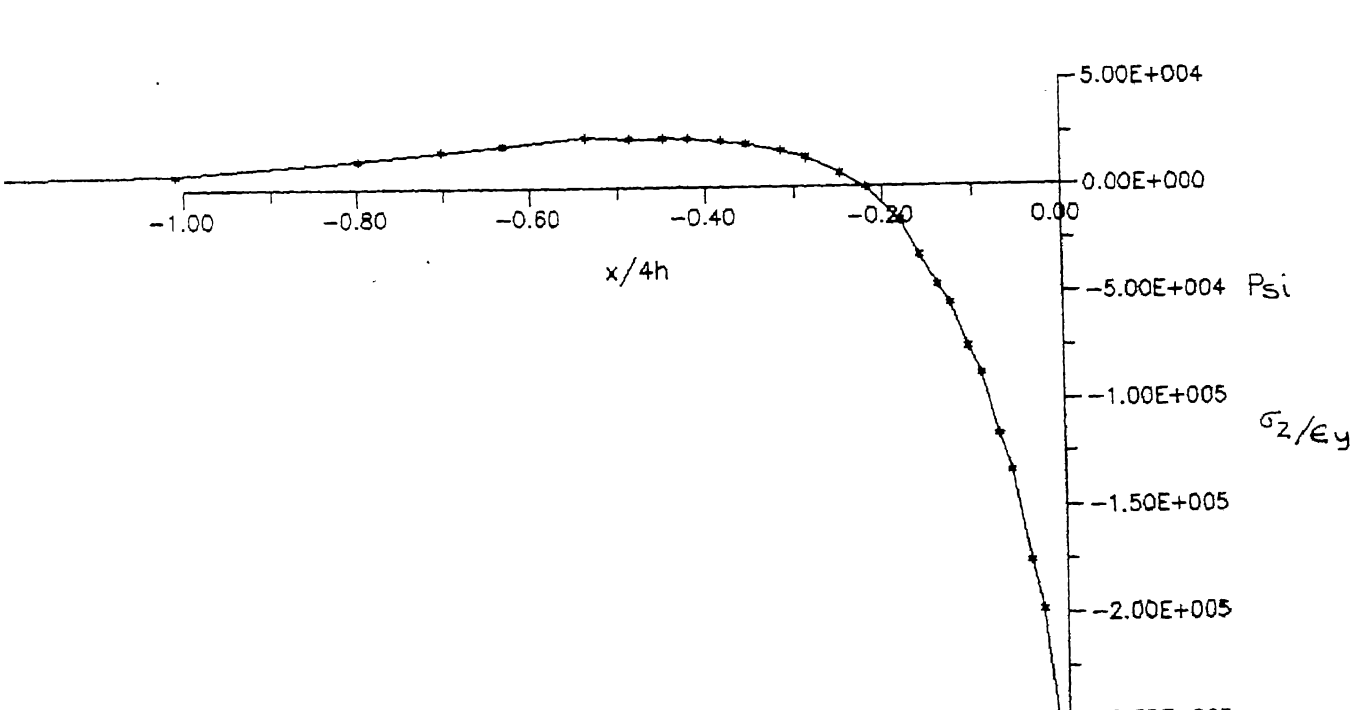

Fig.4.5 Distribution of σ_z of $[+45/-45]_s$ laminated plate at ply interface

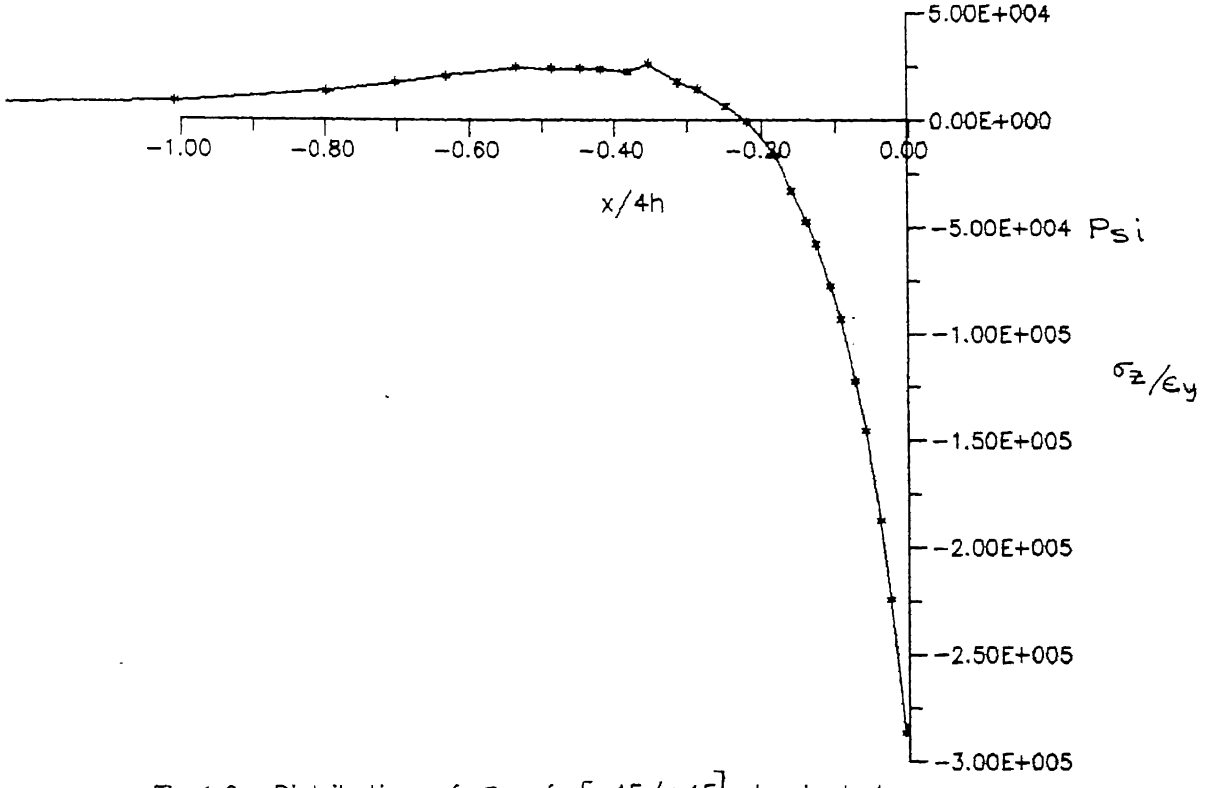

Fig.4.6 Distribution of σ_z of $[-45/+45]_s$ laminated plate at ply interface

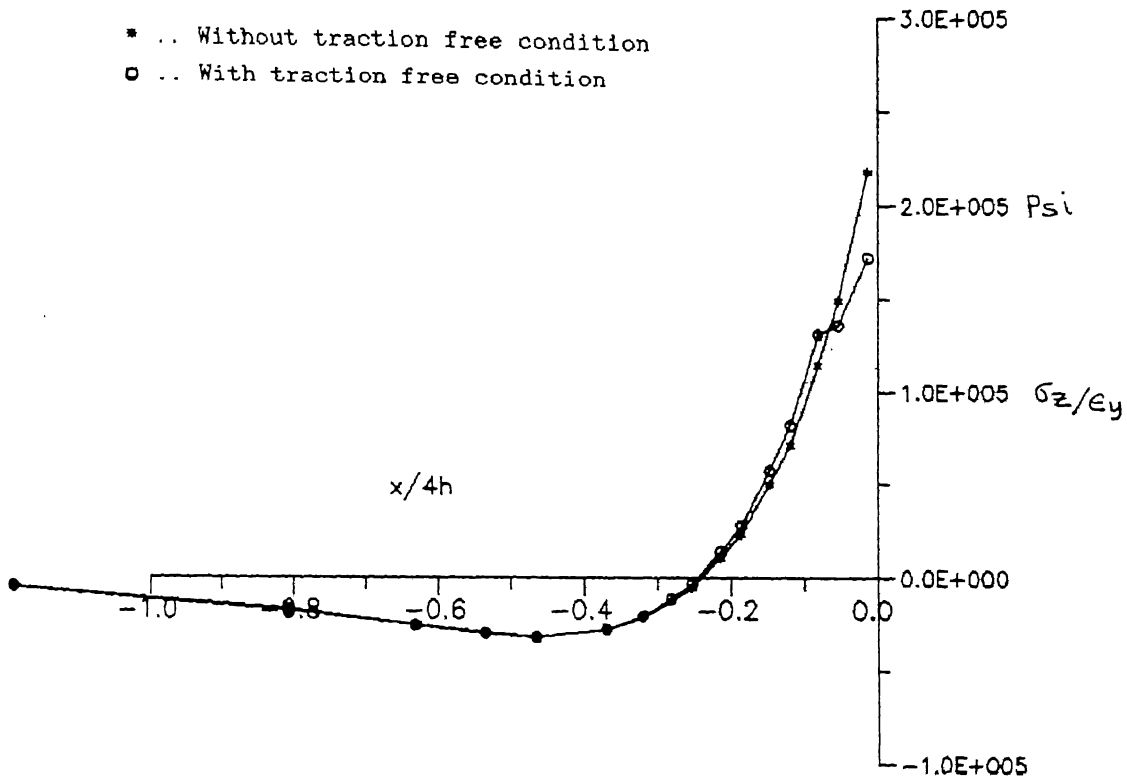

Fig.4.7 Distribution of σ_z of $[0/90]_s$ laminated plate at ply interface

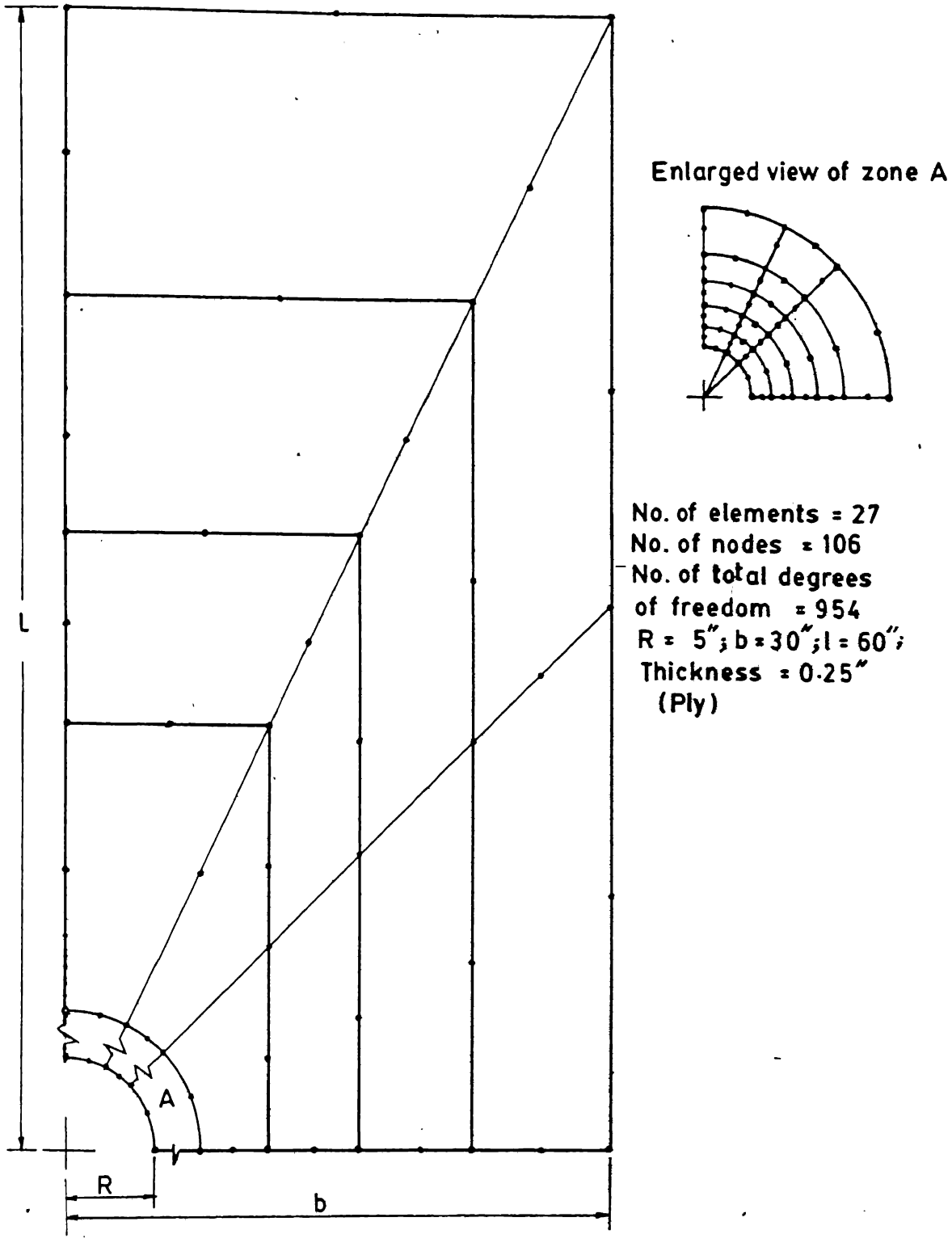

FIG. 4.8 FEM DISCRETIZATION OF LAMINATE PLATE WITH CIRCULAR HOLE

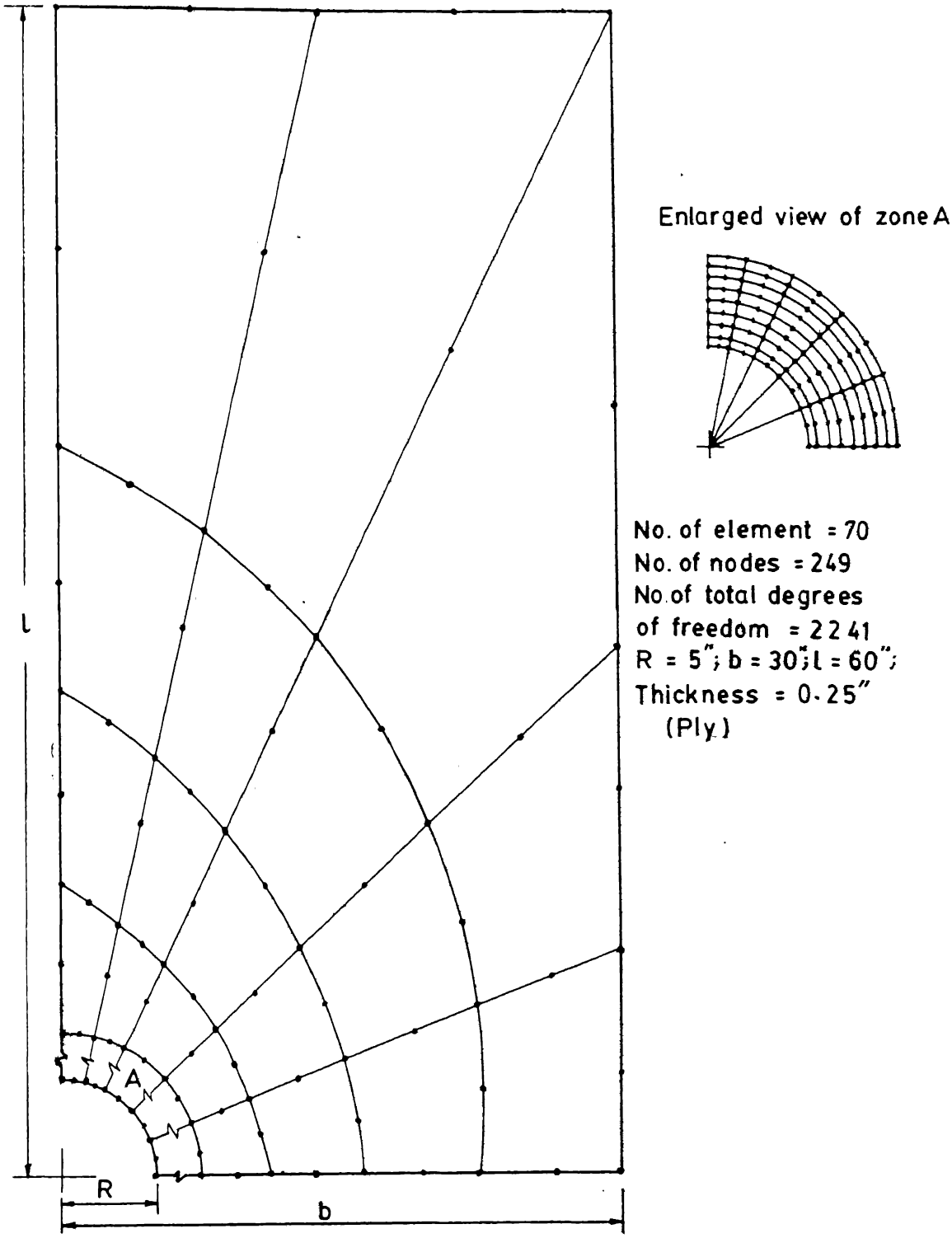

FIG. 4.9 FEM DISCRETIZATION OF LAMINATE PLATE WITH CIRCULAR HOLE

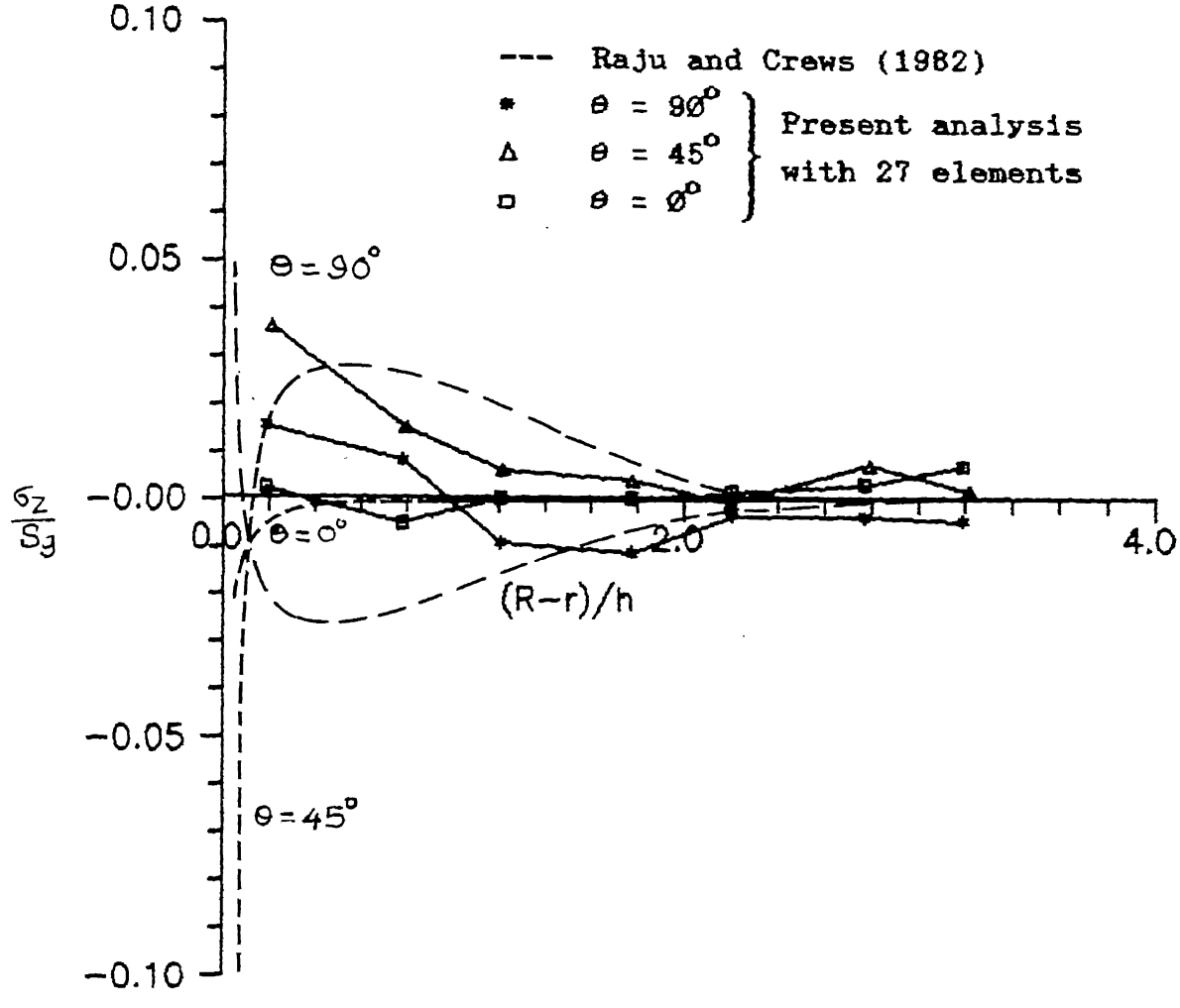

Fig.4.10(a) σ_z radial distribution of $[0/90]_s$ laminated plate with circular hole, at ply interface

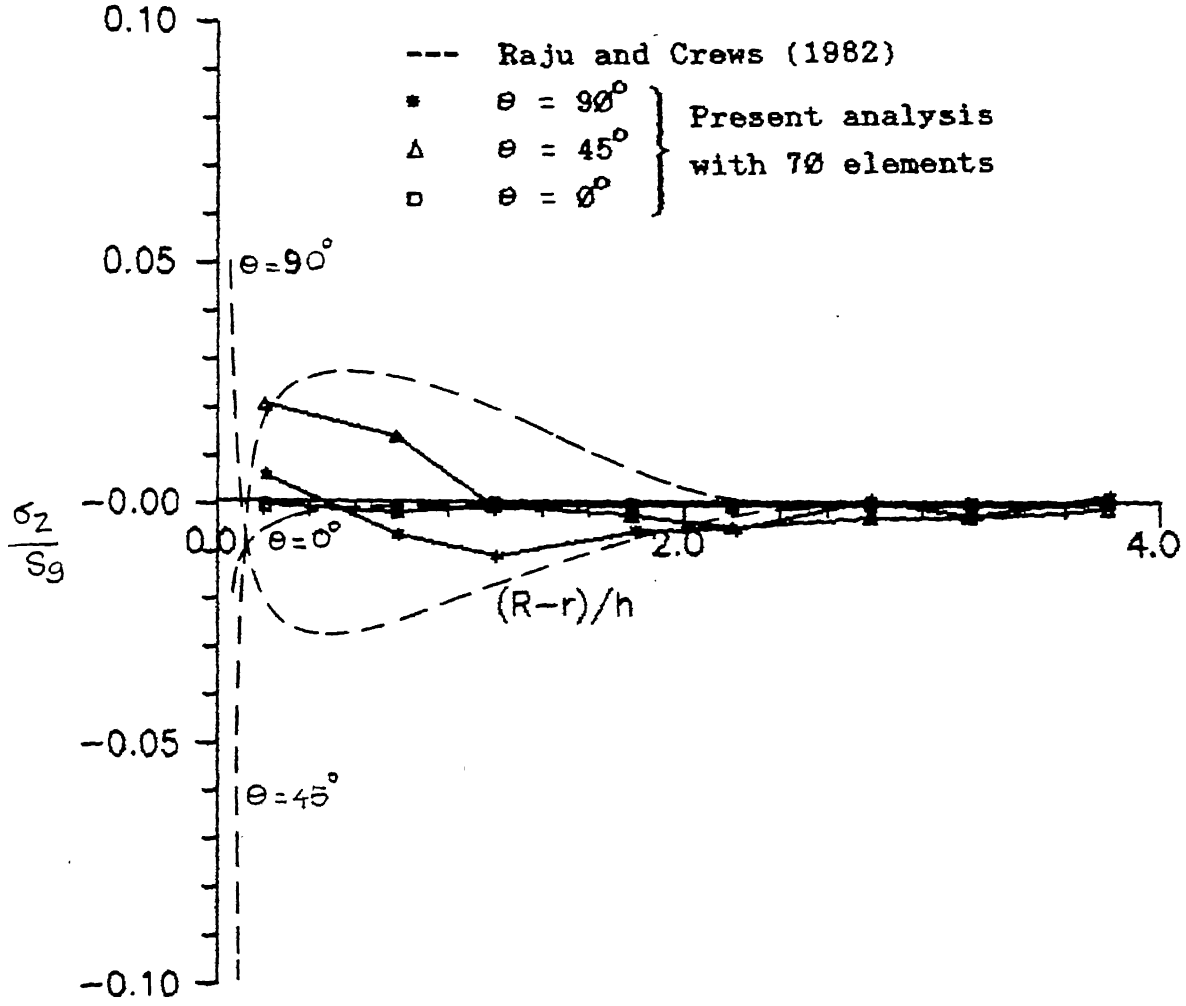

Fig.4.10(b) σ_z radial distribution of 0/90 laminated plate with circular hole, at ply interface

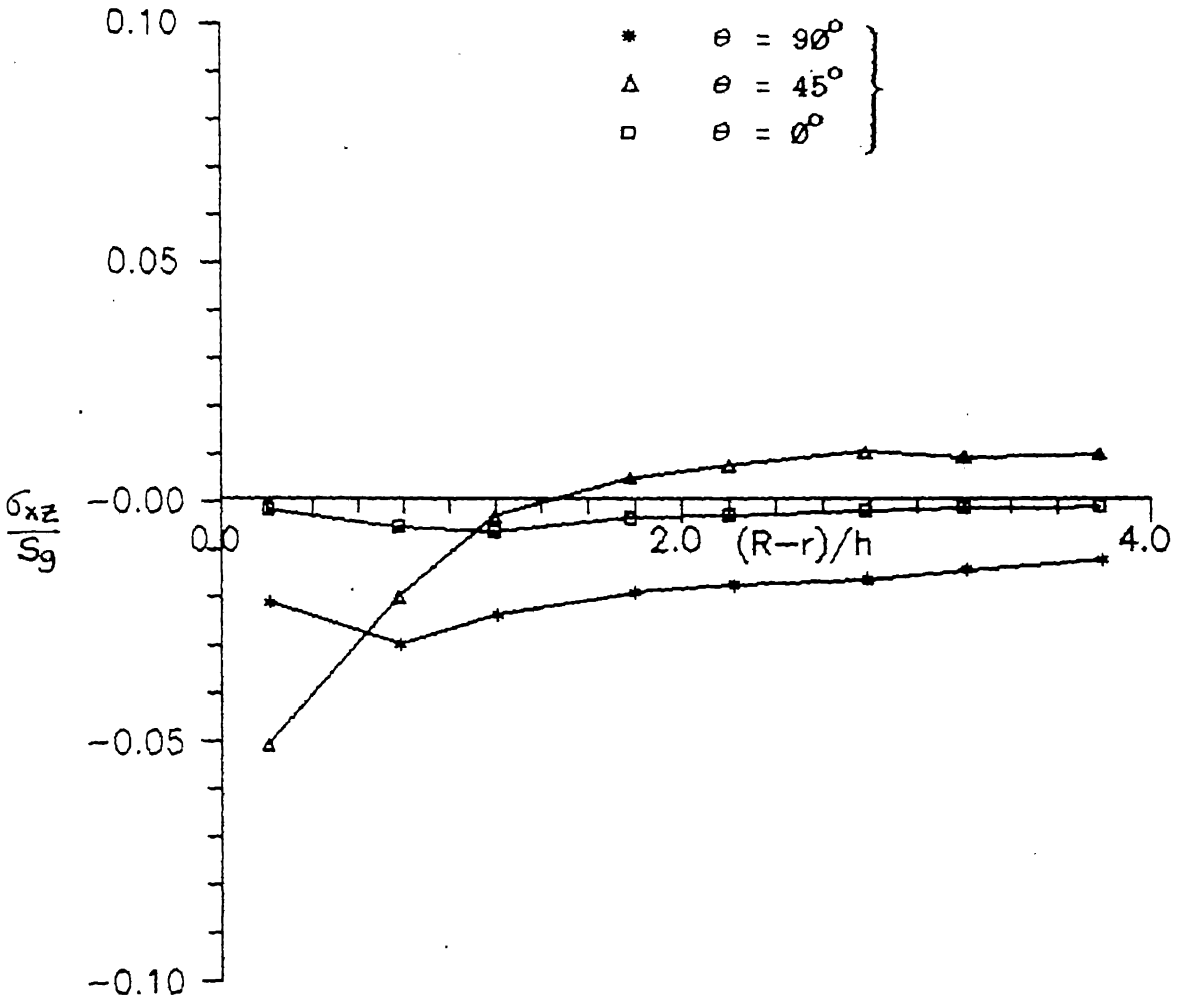

Fig.4.11 σ_{xz} radial distribution of $[0/90]_s$ laminated plate with circular hole, at ply interface

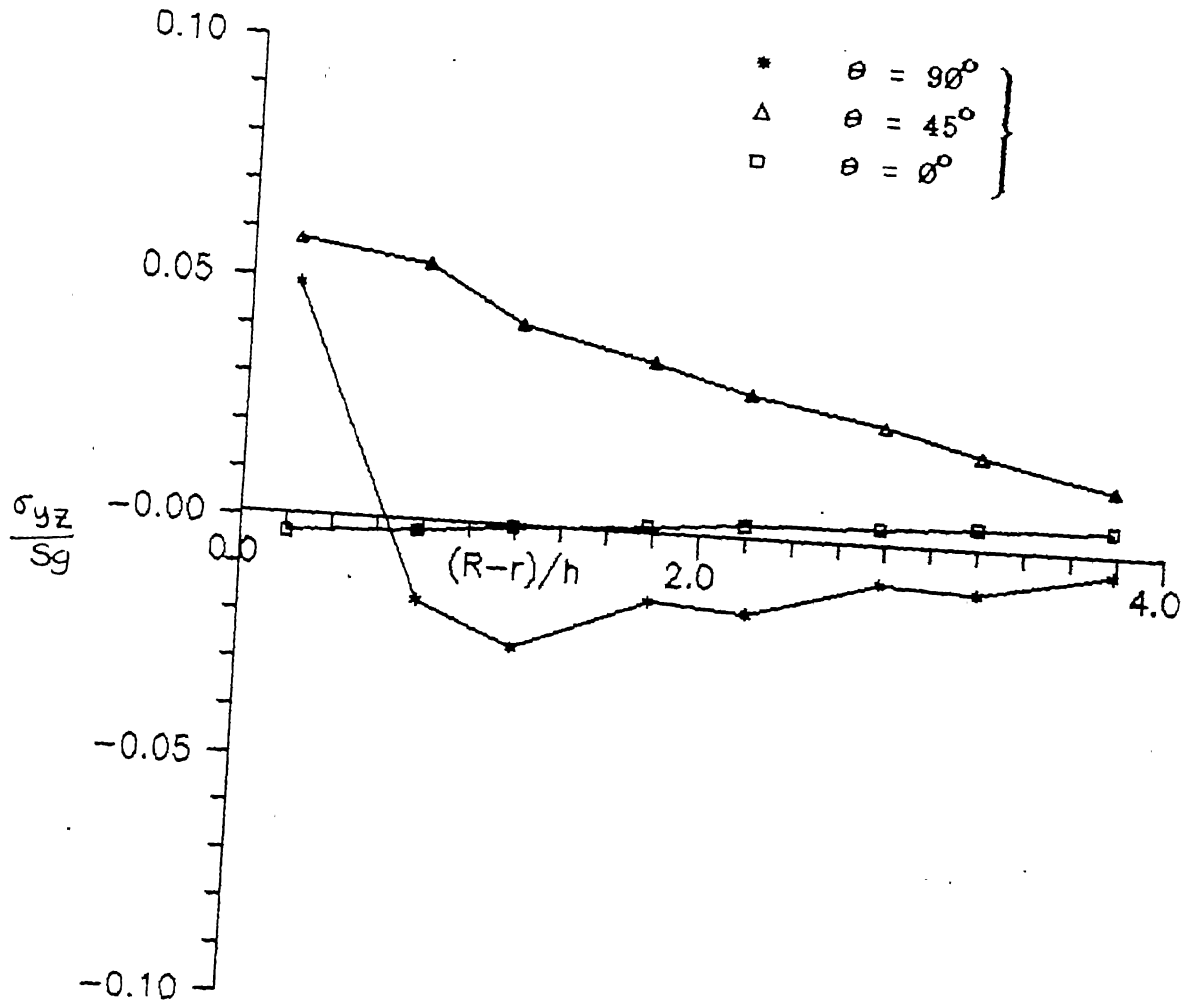

Fig.4.12 σ_{yz} radial distribution of $[0/90]_s$ laminated plate with circular hole, at ply interface

Fig.4.13 σ_z distribution through the laminate thickness of $[0/90]_s$ laminated plate with circular hole

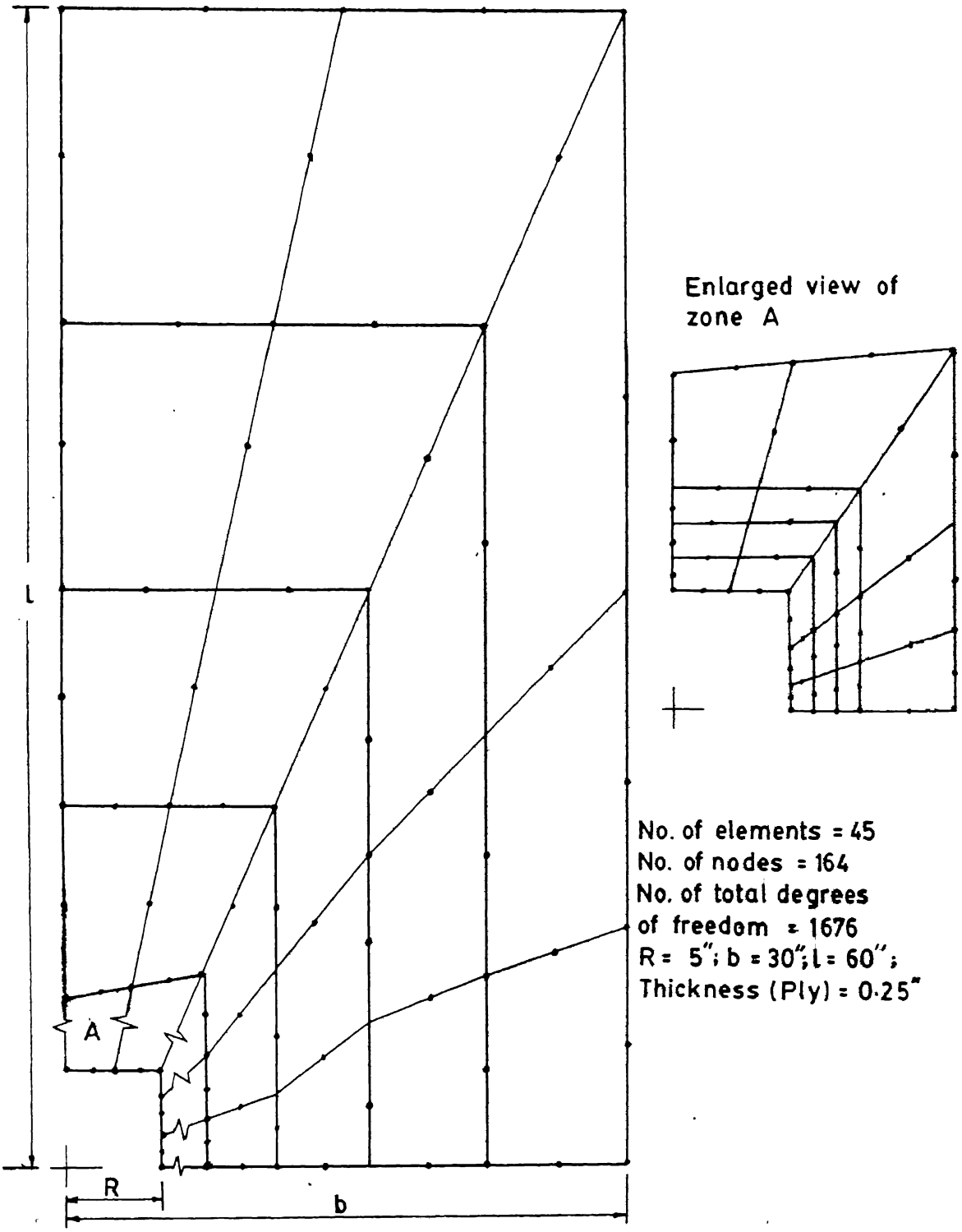

FIG.4.14 FEM DISCRETIZATION OF LAMINATED PLATE WITH SQUARE HOLE

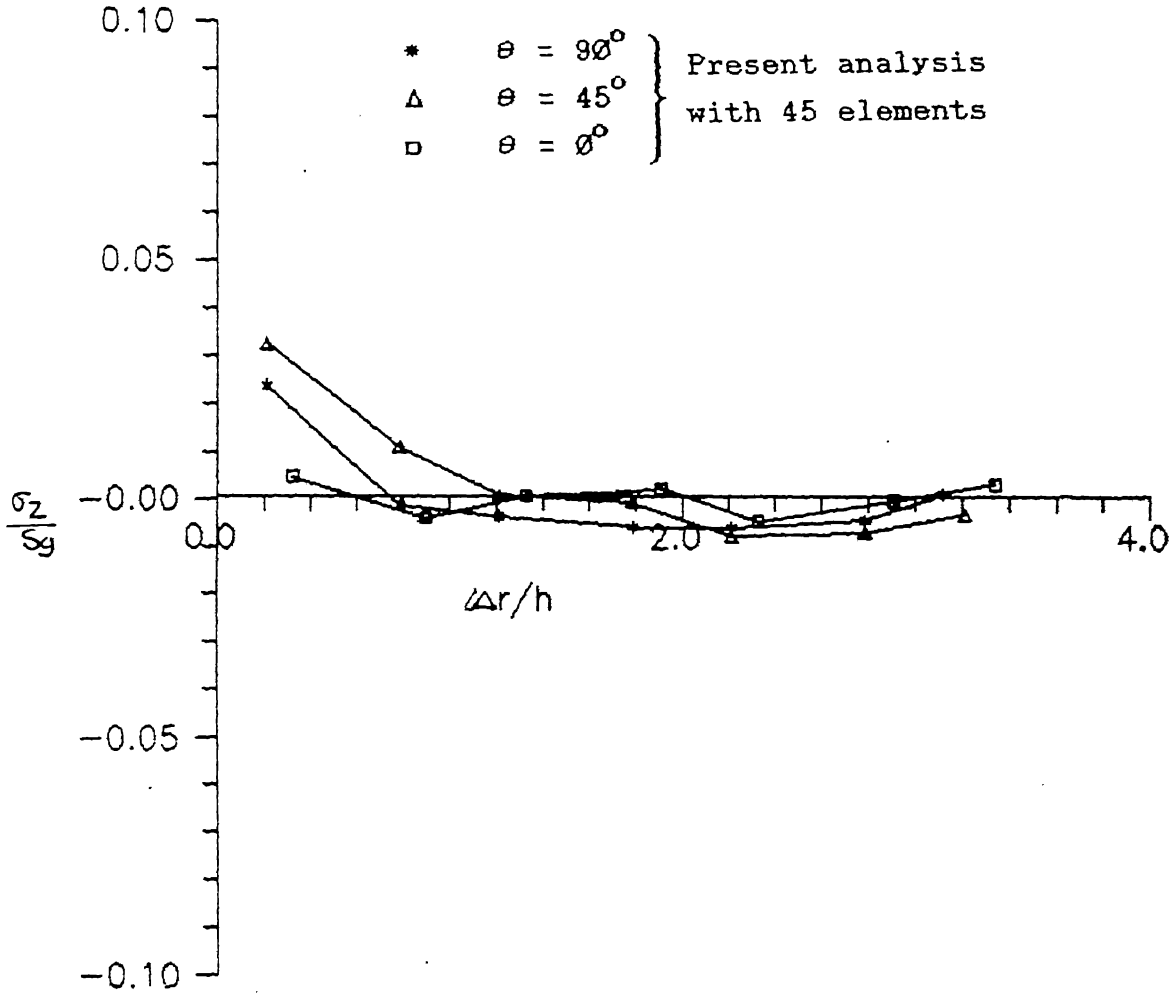

Fig.4.15 σ_z radial ditribution of $[0/90]_s$ laminated plate with square hole at ply interface

CHAPTER V

CONCLUSIONS AND SUGGESTIONS FOR FUTURE WORK

5.1 CONCLUSIONS

In the present work interlaminar stresses near a straight edge, circular hole and square hole boundaries in symmetric composite laminates have been determined. Hybrid finite element method suitable for layered composite media is used for the above purpose. Based on the results and discussion presented in chapter-IV the following conclusions may be drawn:

1) The interlaminar stresses in all the cases are significant near the edge and die down within a distance of laminate thickness from the edge.

2) In the case of circular hole the normal stress σ_z and shear stresses σ_{xz}, σ_{yz} are significant at $\theta = 45^{\circ}$ which may initiate mixed mode delamination.

3) In the case of square hole the above stresses are much more and the mixed mode delamination seems to be very likely.

4) The hybrid finite element method is a very useful and convenient for layered composite media.

5.2 SUGGESTIONS FOR FUTURE WORK

1) Finer mesh be used near the edges to obtain better accuracy.

2) More than two layered-element be used (such as $[\emptyset_2/90\emptyset_2]_s$) to

= 0° the normal stress anywhere in the thickness is more or less zero and at $\theta = 90^{\circ}$ is tensile at the interface and in the top layer, (i.e., 0° layer) whereas the normal stress is tensile in the both the layers and significant at $\theta = 45^{\circ}$.

4.3 EDGE STRESSES NEAR THE SQUARE HOLE BOUNDARY IN SYMMETRIC COMPOSITE LAMINATE

Similar to the analysis of edge stresses near a circular hole in a symmetric laminate, hybrid finite element method analysis is carried out in the case of a $[0/90]_s$ laminate with a square hole. The laminate geometry and material properties are assumed to be same as in the previous case. The finite element discretization of the laminate is shown in Fig. 4.14. The mesh is made finer near the hole and has a total number of 45 elements. The stresses at the interface of 0° and 90° layers is computed as explained in section 4.2.

The interlaminar normal stress, σ_z is shown in Fig. 4.15. The three curves represent the stress variation along the radial lines $\theta = 0^{\circ}$, $\theta = 45^{\circ}$ and $\theta = 90^{\circ}$. Here also, the normal stress at $\theta = 0^{\circ}$ is negligible whereas it has significant positive value near $\theta = 45^{\circ}$ and $\theta = 90^{\circ}$. These values seem to be more than those in the case of circular hole. However, overall the variation is same. Thus square hole seems to have more tendency for delamination.

achieve better stress variation in the thickness direction leading to more efficient interlaminar stress evaluation.

3) New polynomial expressions for the stress assumptions be derived to improve accuracy.

4) Mixed mode delamination theories be used to investigate the actual nature of delamination.

REFERANCES

Agarwal, B.D. and Brouthman, L.J. "Analysis and performance of fibre composites", John Wiley and Sons, New York (1980).

Altus, E., Ratem, A. and Shmeli, M. "Free edge effect in angle-ply laminates - A new finite difference solution", J. Comps. Mater., 14, 21-30 (1980).

Chaudhuri, R.A. and Seide, P. "An approximate semi-analytical method for prediction of interlaminar shear stresses in arbitarily laminated thick plates", Comp. Struct., 25, 627-636 (1987).

Hington, E. and Owen D.R.J., Finite element programming, Academic Press (1970).

Isakson, G. and Levy, A. "Finite element analysis of interlaminar shear fibrous composites", J. Comps. Mater., 5, 273-276 (1971).

Kassapoglou, C. and Lagace, P.A. "An efficient method for calculation of interlaminar stresses in composite materials", ASME J. Appl. Mech., 53, 744-750 (1986).

Lee, J.D. Three dimensional finite element analysis of layered fibre-reinforced composite material", Comp. Struct., 12, 319-339 (1980).

Pagano, N.J. and Pipes, R.B. "The influence of stacking sequence on laminate strength", J. Comps. Mater., 5, 50-57 (1971).

Pagano, N.J. "On the calculation of interlaminar normal stress in composite laminate", J. Comps. Mater., 8, 65-81 (1974).

Pagano, N.J. "Free edge stress fields in composite laminates", Int. J. Solids Struct., 14, 400-406 (1978).

Pian, T.N.H. "Hybrid elements", Int. J. Numer. Methods Engg., 4, 59-78 (1973).

Pipes, R.B. and Pagano, N.J. "Interlaminar stresses in composites under uniform axial extension", J. Comps. Mater., 4, 538-548 (1970).

Pipes, R.B. and Daniel, I.M. "Moire analysis of the interlaminar shear edge effect in laminated composites", J. Comps. Mater., 5, 255-259 (1971).

Pipes, R.B. and Pagano, N.J. "interlaminar stresses in composite laminates - An approximate elasticity solution", ASME J. Appl. Mech., 41, 668-672 (1974).

Puppo, A.H. and Evensen, H.A. "Interlaminar shear in laminated composites under generalized plane stress", J. Comps. Mater., 4, 204 - 220 (1970).

Raju, I.S. and Crews, J.H. "Interlaminar stress singularites at a straight free edge in composite laminates", Comp. Struct., 14, 21-28 (1981).

Raju, I.S. and Crews, J.H. "Three dimensional analysis of $[0/90]_s$ and $[90/0]_s$ laminates with a central circular hole", Comps. Tech. Review, 4, 116-124, (1982).

Rohwer, K. "On the determination of edge stresses in layered composites", Nucl. Engg. and Des., 70, 57-65 (1982).

Rybicki, E.F. "Approximate three dimensional solutions for symmetric laminates under inplane loading", J. Comps. Mater. , 5, 354-360 (1971).

Spilker, R.L. and Chow, S.C. "Edge effect in symmetric composite laminates: Importance of satisfying the traction-free-edge condition", J. Comps. Mater., 14, 2-20 (1980).

Spilker, R.L. and Munir, N.I. "The hybrid stress model for thin plates", Int. J. Num. Method Engg., 15, 1239-1260 (1980).

Splilker R.L. and Munir, N.J. "A Serendipity cubic displacement stress element for thin and moderately thick plates", Int. J. Num. Method Engg., 15, 1261-1278 (1980).

Spilker, R.L. "A hybrid stress formulation for thick mulatilayered laminates", Comp. Struct. 11, 507-514 (1980).

Spilker, R.L. "Hybrid-stress eight-node elements for thin and thick multilayer laminated plates", Int. J. Num. Method Engg., 18, 801-828 (1982).

Tang S. "Interlaminar stresses of uniformly loaded rectangular composite plates", J. Comps. Mater., 10, 69-78 (1976).

Tang S. "Interlaminar stresses around circular cutouts in composite plates under tension", AIAA Journal, 15, 1631-1637 (1977).

Wang, A.S.D. and Crossmen, F.W. "Some new results on edge effects in symmetric composite laminates", J. Comps. Mater. 11, 92-106 (1977).

Wang, J.T.S. and Dickson, J.N. "Interlaminar stresses in symmetric composite laminates", J. Comps. Mater., 12, 390-402 (1978).

Wang, S.S.and Yuan, F.K. "A singular hybrid finite element analysis of boundary layer stresses in composite laminates", Int. J. Solid Stuct., 19, 825-837 (1983).

Zienckiewicz, O.C., "The finite element method", Tata McGrawHill Publishing Co. Ltd. (New Delhi), 1977.

APPENDIX-A

The σ-β stress assumption [Spilker (1982)] is given below:

$$\sigma_x^i = \beta_{16} + [\tfrac{1}{2}(\beta_1 - \beta_{59}) - \beta_{26}]x + \beta_{27}\, y + [\tfrac{1}{4}(\beta_2 - \beta_{54}) - \tfrac{1}{2}\beta_{28}]x^2 + [\tfrac{1}{2}(\beta_3 - \beta_{55}) - 2\beta_{29}]xy + \beta_{18}\, y^2 + [\tfrac{1}{6}(\beta_4 - \beta_{56}) - \tfrac{1}{3}\beta_{31}]x^3 + [\tfrac{1}{4}(\beta_5 - \beta_{57}) - \beta_{32}]x^2y + [\tfrac{1}{2}(\beta_6 - \beta_{58}) - 3\beta_{33}]xy^2 + \beta_{19}\, y^3 + \zeta\Big\{\beta_{34} + \beta_{35}x + \beta_{36}y + \beta_{37}x^2 + \beta_{38}xy + \beta_{39}y^2 + [-\tfrac{3}{4}(\beta_{67} - \beta_{15} + \beta_5 + \beta_{57} + 2\beta_{12} + 2\beta_{64})]x^2y + \beta_{40}xy^2\Big\}$$

$$\sigma_y^i = \beta_{20} + \beta_{21}x + [\tfrac{1}{2}(\beta_7 - \beta_{59}) - \beta_{25}]y + \beta_{22}x^2 + [\tfrac{1}{2}(\beta_8 - \beta_{60}) - 2\beta_{27}]xy + [\tfrac{1}{4}(\beta_9 - \beta_{61}) - \tfrac{1}{2}\beta_{28}]y^2 + \beta_{29}x^3 + [\tfrac{1}{2}(\beta_{10} - \beta_{62}) - 3\beta_{30}]x^2y + [\tfrac{1}{4}(\beta_{11} - \beta_{63}) - \beta_{31}]xy^2 + [\tfrac{1}{6}(\beta_{12} - \beta_{64}) - \tfrac{1}{3}\beta_{32}]y^3 + \zeta\Big\{\beta_{41} + \beta_{42}x + \beta_{43}y + \beta_{44}x^2 + \beta_{45}xy + \beta_{46}y^2 + \beta_{47}x^2y + [-\tfrac{3}{4}(\beta_{66} - \beta_{14} + 2\beta_4 + 2\beta_{56} + \beta_{11} + \beta_{63})]xy^2\Big\}$$

$$\sigma_{xy}^i = \beta_{24} + \beta_{25}x + \beta_{26}y + \beta_{27}x^2 + \beta_{28}xy + \beta_{29}y^2 + \beta_{30}x^3 + \beta_{31}x^2y + \beta_{32}xy^2 + \beta_{33}y^3 + \zeta\Big\{\beta_{48} + \beta_{49}x + \beta_{50}y + \beta_{51}x^2 + [-\tfrac{3}{4}(\beta_{65} - \beta_{13} + \beta_2 + \beta_{54} + \beta_9 + \beta_{61}) - (\beta_{37} + \beta_{36})]xy + \beta_{52}y^2\Big\}$$

$$\sigma_{yz}^i = \bar{t}_i\Big\{\tfrac{1}{2}(1-\zeta)(\beta_7 + \beta_8 x + \beta_{10}x^2 + \beta_{12}y^2) + \tfrac{1}{8}(1-\zeta)(1-3\zeta)\beta_9 y + \tfrac{1}{4}(1-\zeta)(-1-3\zeta)\beta_{11}xy + \tfrac{1}{2}(1+\zeta)(\beta_{59} + \beta_{60}x + \beta_{62}x^2 + \beta_{64}y^2) + \tfrac{1}{8}(1+\zeta)(1+3\zeta)\beta_{61}y + \tfrac{1}{4}(1+\zeta)(-1+3\zeta)\beta_{63}xy + \tfrac{1}{2}(1-\zeta^2)\Big\{(\beta_{43} + \beta_{49}) + (\beta_{45} + 2\beta_{51})x + [-\tfrac{3}{4}(\beta_{65} - \beta_{13} + \beta_2 + \beta_{54}) + (\beta_{46} - \beta_{37})]y + \beta_{47}x^2 + [-\tfrac{3}{2}(\beta_{66} - \beta_{14}) - 3(\beta_4 + \beta_{56})]xy\Big\}\Big\}$$

$$\sigma^{i}_{xz} = \bar{t}_i\Big\{\tfrac{1}{2}(1-\zeta)(\beta_1+\beta_3 y+\beta_4 x^2+\beta_6 y^2)+\tfrac{1}{8}(1-\zeta)(1-3\zeta)\beta_2 x$$
$$+\tfrac{1}{4}(1-\zeta)(-1-3\zeta)\beta_5 xy+\tfrac{1}{2}(1+\zeta)(\beta_{58}+\beta_{55}y+\beta_{56}x^2+$$
$$\beta_{58}y^2)+\tfrac{1}{8}(1+\zeta)(1+3\zeta)\beta_{54}x+\tfrac{1}{4}(1+\zeta)(-1+3\zeta)\beta_{57}xy$$
$$+\tfrac{1}{2}(1-\zeta^2)\Big\{(\beta_{35}+\beta_{50})+[-\tfrac{3}{4}(\beta_{66}-\beta_{19}+\beta_{9}+\beta_{61})+(\beta_{37}$$
$$-\beta_{46})]x+(\beta_{38}+2\beta_{52})y+[-\tfrac{3}{2}(\beta_{67}-\beta_{15})-3(\beta_{12}+\beta_{64})]xy$$
$$+\beta_{40}y^2\Big\}\Big\}$$

$$\sigma^{i}_{z} = \bar{t}^2_i\Big\{\tfrac{1}{4}(1-\zeta)^2(2+\zeta)(\beta_{13}+\beta_{14}x+\beta_{15}y)+\tfrac{1}{4}(1+\zeta)^2(2-\zeta)$$
$$(\beta_{65}+\beta_{66}x+\beta_{67}y)-\tfrac{1}{4}(1-\zeta)^2(1+\zeta)[(\beta_2+\beta_9)+(2\beta_4+$$
$$\beta_{11})x+(\beta_5+2\beta_{12})y]+\tfrac{1}{4}(1-\zeta)(1+\zeta)^2[(\beta_{54}+\beta_{61})+$$
$$(2\beta_{56}+\beta_{69})x+(\beta_{57}+2\beta_{64})y]\Big\}$$

APPENDIX-B

The standard shape functions used for 8-noded qudrilateral elements are:

$$N_1(\xi,\eta) = (1 - \xi)(1 - \eta)(-1 - \xi - \eta)/4$$

$$N_2(\xi,\eta) = (1 - \xi^2)(1 - \eta)/2$$

$$N_3(\xi,\eta) = (1 + \xi)(1 - \eta)(-1 + \xi - \eta)/4$$

$$N_4(\xi,\eta) = (1 - \xi)(1 - \eta^2)/2$$

$$N_5(\xi,\eta) = (1 + \xi)(1 + \eta)(-1 + \xi + \eta)/4$$

$$N_6(\xi,\eta) = (1 - \xi^2)(1 + \eta)/2$$

$$N_7(\xi,\eta) = (1 - \xi)(1 + \eta)(-1 - \xi + \eta)/4$$

$$N_8(\xi,\eta) = (1 - \xi)(1\ \eta^2)/2$$